nature structural & molecular biology

The ATPase domain of ISWI is an autonomous nucleosome remodeling machine

Felix Mueller-Planitz[1,2], Henrike Klinker[1,2], Johanna Ludwigsen[1,2] & Peter B Becker[1,2]

ISWI slides nucleosomes along DNA, enabling the structural changes of chromatin required for the regulated use of eukaryotic genomes. Prominent mechanistic models imply cooperation of the ISWI ATPase domain with a C-terminal DNA-binding function residing in the HAND-SANT-SLIDE (HSS) domain. Contrary to these models, we show by quantitative biochemical means that all fundamental aspects of nucleosome remodeling are contained within the compact ATPase module of *Drosophila* ISWI. This domain can independently associate with DNA and nucleosomes, which in turn activate ATP turnover by inducing a conformational change in the enzyme, and it can autonomously reposition nucleosomes. The role of the HSS domain is to increase the affinity and specificity for nucleosomes. Nucleosome-remodeling enzymes may thus have evolved directly from ancestral helicase-type motors, and peripheral domains have furnished regulatory capabilities that bias the remodeling reaction toward different structural outcomes.

Chromatin organization endows eukaryotic genomes with stability and regulates gene expression. DNA within chromatin is spooled around histone proteins, forming nucleosomes. Arrays of nucleosomes are further folded to accommodate the genome in the nuclear volume. Tight packaging inevitably leads to the occlusion of DNA sequences that can no longer be accessed by regulatory proteins. However, chromatin has to be dynamic to permit cells to respond to environmental or developmental challenges. Crucial to a dynamic and regulated use of the genome are the actions of ATP-consuming nucleosome-remodeling enzymes[1,2].

Nucleosome-remodeling enzymes use energy from ATP hydrolysis to weaken or disrupt histone-DNA contacts in the otherwise extremely stable nucleosome particle. They thereby catalyze histone exchange, partial or complete nucleosome disassembly and formation of new nucleosomes or repositioning of existing ones. The precise outcome of a remodeling reaction is frequently determined by regulatory subunits that associate with the ATPase[2–5].

The ATPase domains of all nucleosome-remodeling complexes are conserved and distantly related to superfamily 2 (SF2) DNA helicases. On the basis of similarity of their ATPase domain sequences, all known or presumed nucleosome-remodeling enzymes constitute 24 subfamilies[4,6]. Despite this complexity, it is becoming clear that the remodeling enzymes studied to date are related in structure and mechanism. Deciphering the fundamental mechanism of a basic remodeling reaction remains an important goal[2–5].

Most insight into the mechanism of nucleosome remodeling has been obtained by studying representatives of three subfamilies of remodelers: ISWI, Snf2 and Chd1. They all slide nucleosomes along DNA, and although differences have been noted[7,8], they share a strategic interaction site on the nucleosome. Their ATPase 'motor' domain engages the nucleosomal DNA about two helical turns off the nucleosomal dyad at superhelix location 2 (SHL2)[9–11]. This site is characterized by structural variability of the histone-DNA interactions. It can accommodate a gain or loss of one base pair (bp), a feature that could be exploited during the remodeling reaction[12–14]. Furthermore, the histone H4 N terminus, which is mechanistically involved in remodeling reactions catalyzed by ISWI and Chd1, emanates from the nucleosome core around SHL2 (refs. 15–19). At SHL2, the ATPase domain is thought to translocate on DNA in accord with its helicase ancestry[9,20,21]. The ATPase domain may thereby force additional DNA into the nucleosome, change the twist in the DNA or otherwise perturb histone-DNA contacts[2,4,22].

In several cases it was observed that successful remodeling required accessory domains in addition to the ATPase. These domains are thought to provide the appropriate mechanical or topological context for remodeling. For ISWI-type enzymes, the C terminus harbors a DNA-binding module in the form of the HSS domain (**Fig. 1a**). Deletion of the HSS domain markedly reduced the ability of *Drosophila* ISWI to associate with and remodel nucleosomes[23]. Subsequent cross-linking and cryo-EM studies with the ISWI orthologs in yeast revealed interactions of the HSS domain with DNA flanking the nucleosome, so-called linker or extranucleosomal DNA[24,25]. Deletion of this DNA diminished not only the binding affinity but also the ATP turnover and the remodeling capacity of ISWI[26,27].

These results collectively support models in which the nucleosomal contacts made by the ISWI ATPase and HSS modules delimit a topological domain of nucleosomal DNA. Conceivably, a conformational change between the ATPase and the HSS modules, mediated by a

[1]Adolf Butenandt Institut, Ludwig-Maximilians-Universität, Munich, Germany. [2]Center for Integrated Protein Science Munich, Ludwig-Maximilians-Universität, Munich, Germany. Correspondence should be addressed to F.M.-P. (Felix.Mueller-Planitz@med.uni-muenchen.de) or P.B.B. (pbecker@med.uni-muenchen.de).

Received 3 May; accepted 1 November; published online 2 December 2012; doi:10.1038/nsmb.2457

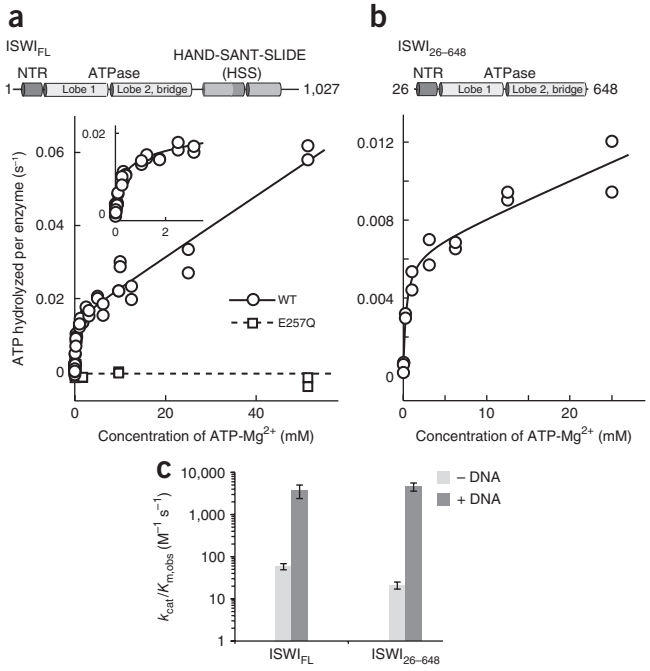

Figure 1 Steady-state ATP hydrolysis. (**a**,**b**) ATP concentration dependence of ATP turnover by DNA-free ISWI$_{FL}$ (**a**) and ISWI$_{26–648}$ (**b**), both 4 μM. The response was biphasic, with the first phase completed with submillimolar concentrations of ATP (**a**, inset). Steady-state ATPase parameters extracted from fits (lines) are listed in **Table 1**. Domain schematics for ISWI$_{FL}$ and ISWI$_{26–648}$ are shown on top. In addition to wild-type (WT), an ATPase-deficient mutant (E257Q) was used as a negative control in **a**. (**c**) Strong stimulation of ATP hydrolysis of ISWI$_{FL}$ and ISWI$_{26–648}$ by saturating concentrations of a 39-bp-long DNA duplex (80 to 400 nM). The assays were performed with 100 mM Mg^{2+}; similar results were obtained in a buffer containing lower Mg^{2+} concentrations or varying enzyme concentrations (**Supplementary Table 1** and **Supplementary Fig. 2a,b** and data not shown).

'hinge' that connects the two, may destabilize the DNA-histone contacts in this domain and pull linker DNA into the nucleosome[16,18]. The excess DNA would initially bulge out from the histone surface. Eventually it may escape from the other side of the nucleosome and re-form the canonical nucleosome structure at a different position on DNA.

This model predicts that the HSS domain plays an integral part during the remodeling reaction. Underscoring its importance, deletion of a related domain in Chd1 strongly reduced the overall remodeling efficiency[28]. Unexpectedly, a different study concluded that deletion of the DNA-binding module in the C terminus of Chd1 does not completely abolish the nucleosome sliding activity. Rather, the C terminus was suggested to affect the directionality of the process[11]. Thus, the DNA-binding domain may not be essential for the remodeling process as such. It might instead determine the overall outcome of the remodeling reaction, either the direction of nucleosome sliding[11] or the positioning of the substrate nucleosome in the context of nucleosome spacing[28]. This conclusion is not readily compatible with the hinge model, which was mainly derived from studies on ISWI-type enzymes. Do these studies reveal a fundamental difference between ISWI- and Chd1-type remodelers with respect to their use of binding domains for linker DNA? How can ATP hydrolysis–driven conformational changes be productive in the absence of the main linker DNA–binding domain?

We set out to address these issues in the context of *Drosophila* ISWI. Our quantitative analysis reveals two ATPase domain conformations, which drastically differ in their catalytic competency. Nucleic acids induce a change of conformation, thereby activating the enzyme. Furthermore, we show that the ATPase domain has an intrinsic ability to bind nucleosomes, to functionally interact with the H4 N terminus and to remodel nucleosomes. Accessory domains in chromatin remodelers may thus have evolved to regulate an autonomous basic remodeling module. Our data place firm limits on the mechanistic models of nucleosome remodeling and favor models in which the ATPase domain performs the fundamental steps involved in remodeling, such as breaking histone-DNA contacts and moving nucleosomes, whereas the HSS domain fulfills auxiliary duties, such as increasing the affinity and specificity for nucleosomes.

RESULTS

The ATPase domain adopts different conformations in solution

The ATPase activity of ISWI is activated by free and nucleosomal DNA[23,29]. To dissect this effect in a quantitative manner, we obtained highly purified enzyme preparations by using an optimized purification protocol that included affinity, ion-exchange and size-exclusion chromatography. Further purification did not affect the results.

We first measured ATP turnover by unliganded ISWI and determined the reaction velocities for varying ATP concentrations. Whereas enzymes typically show a simple saturation behavior with increasing substrate concentrations, ISWI featured a more complex biphasic response. After an initial rise of the reaction velocity with increasing ATP concentrations, the curve entered a second phase and continued to rise until at least 50 mM of ATP (**Fig. 1a**).

The two phases of the curve indicated that different enzyme populations existed with strongly differing observed Michaelis ($K_{m,obs}$) values. We hypothesized that these populations may correspond to ISWI molecules in different conformations. Kinetic and thermodynamic modeling confirmed that this scenario could indeed account for the data (**Supplementary Fig. 1**).

However, the biphasic ATPase response could also be due to a number of trivial reasons. Most importantly, we ruled out a contaminating ATPase being responsible for one of the two phases by analyzing a point mutant with an amino acid change in the Walker B motif of the ISWI ATPase domain (E257Q), that prevents ATP hydrolysis. Although this mutant was expressed at similar levels and prepared in the same way as the wild type, we could not detect any ATP hydrolysis for this mutant (**Fig. 1a**). We have ruled out additional scenarios, such as enzyme dimerization and contamination with DNA, that could, in principle, explain the unusual shape of the curve (discussed in **Supplementary Note**; **Supplementary Fig. 2a**,**b**).

According to prominent models of ISWI function, the HSS and ATPase domains intimately cooperate during nucleosome remodeling[2–4,24,30]. In this scenario the HSS domain might be expected to directly influence ATP hydrolysis. We tested this hypothesis by truncating ISWI in a poorly conserved region that separates the ATPase domain from the HSS domain (**Fig. 1b**). Our construct spanned a conserved N-terminal region (NTR; **Supplementary Fig. 3**), both ATPase lobes and the 'bridge' at the C-terminal end, which is conserved between ISWI and Chd1 remodelers and docks against both ATPase lobes[31,32]. In most experiments, we used a construct that lacked nonconserved amino acids at the N terminus, spanning amino acids 26–648 (ISWI$_{26–648}$). We repeated a number of experiments with ISWI$_{1–697}$, which also included less-conserved regions on both termini.

Table 1 Steady-state ATPase parameters[a]

		$ISWI_{FL}$			$ISWI_{26–648}$		
		$k_{cat}/K_{m,obs}$ (M^{-1} s^{-1})	$k_{cat,obs}$ (s^{-1})	$K_{m,obs}$ (mM)	$k_{cat}/K_{m,obs}$ (M^{-1} s^{-1})	$k_{cat,obs}$ (s^{-1})	$K_{m,obs}$ (mM)
– DNA	Phase 1	60 ± 10	0.014 ± 0.004	0.24 ± 0.03	21 ± 3*	0.007 ± 0.002	0.36 ± 0.02*
	Phase 2	NA	>0.046	>50	NA	>0.02	>25
+ DNA		3,700 ± 900*	0.51 ± 0.09	0.15 ± 0.05	4,100 ± 900*	1.0 ± 0.1	0.25 ± 0.01

[a]Values were measured in reaction buffer containing 100 mM Mg^{2+}. Where indicated (asterisks), errors are minimum and maximum values of two independent measurements. Otherwise, errors are s.d. of at least three independent measurements. DNA reactions contained saturating concentrations of a 39-bp DNA duplex. NA, Not applicable.

As in the case with full-length ISWI ($ISWI_{FL}$), the ATP concentration dependencies of unliganded $ISWI_{26–648}$ and $ISWI_{1–697}$ were biphasic, which suggested that the two conformations involve the ATPase domain (**Fig. 1b** and data not shown). Unexpectedly, steady-state ATPase parameters ($k_{cat}/K_{m,obs}$, $k_{cat,obs}$ and $K_{m,obs}$) differed by less than three-fold between the three enzymes (**Fig. 1** and **Table 1** and data not shown). This similarity attested to the integrity of the two truncated proteins and showed that the C terminus did not substantially influence ATP hydrolysis, at least when no DNA ligand was bound.

DNA ligands strongly influence the ATP hydrolysis mechanism

To test how DNA binding affected the catalytic parameters, we repeated the analyses in the presence of a 39-bp-long DNA duplex. Varying the length of the DNA from 19 to ~3,000 bp did not considerably affect the $k_{cat,obs}$ (below and data not shown). In contrast to the ligand-free enzyme, DNA-bound $ISWI_{FL}$ exhibited standard Michaelis-Menten–type kinetics (data not shown). Furthermore, DNA strongly stimulated $k_{cat}/K_{m,obs}$ (61-fold; **Fig. 1c** and **Table 1**).

Like stimulation by DNA, stimulation by chromatin abolished the biphasic response to the ATP concentration (data not shown). Relative to DNA, chromatin binding increased the affinity for nucleotides by six-fold (**Supplementary Fig. 4**). In addition, $k_{cat,obs}$ increased by 4- to 14-fold, depending on the enzyme concentration (**Supplementary Fig. 2c** and **Supplementary Table 1**; here we employed lower Mg^{2+} concentrations to prevent aggregation of chromatin). This dependence of $k_{cat,obs}$ on the enzyme concentration is consistent with binding of two functionally interacting ISWI molecules per nucleosome, as previously suggested (**Supplementary Fig. 2d,e**)[33].

DNA binding to the ATPase domain activates ATP hydrolysis

Nucleic acids typically directly bind the ATPase domain of SF2 helicases[34,35]. Using the $ISWI_{26–648}$ construct, we confirmed in a double-filter binding assay that the ATPase domain of ISWI indeed harbors a DNA-binding site (**Supplementary Fig. 5**). Consistent with its DNA-binding function[23–25,36], the HSS domain increased the DNA affinity by 20-fold.

DNA could, in principle, activate ATP hydrolysis by binding to either of the two binding sites or to both. Whereas nucleic acids often directly bind and stimulate the ATPase activity of SF2 helicases[34,35], we previously suggested that it was DNA binding to the HSS domain that conferred most DNA stimulation[23]. However, at that time we did not account for the reduced DNA affinity when the HSS domain is missing. To differentiate between the two sites and to probe their involvement in the regulation of ATP turnover, we titrated DNA to the ISWI constructs that lacked the HSS domain and measured ATP turnover. DNA was a potent activator of ATP hydrolysis of $ISWI_{26–648}$ and $ISWI_{1–697}$ (**Fig. 1c** and data not shown). Overall, their ATPase parameters were strikingly similar to those of $ISWI_{FL}$, indicating that DNA binding at the ATPase domain, not the HSS domain, drives the stimulation (**Table 1**).

DNA binding affects the conformation of the ATPase domain

To test whether DNA binding activated ATP turnover by triggering a conformational change in the ATPase domain, as seen for evolutionarily related proteins[37], we turned to limited proteolysis experiments. Consistent with a structural change, limited digestion with trypsin led to a different cleavage pattern and a substantially faster cleavage of $ISWI_{26–648}$ in the presence of DNA (**Fig. 2a**). A different protease (GluC) and partial trypsin digests of $ISWI_{FL}$ yielded analogous results (data not shown).

Additional proteolysis experiments firmly ruled out that the different cleavage pattern was simply due to occlusion of the predominant cleavage sites by DNA. From a comparison of the electrophoretic mobility of proteolytic fragments obtained with trypsin, which cleaves at lysines and arginines, and LysC, which is specific for lysine, we concluded that the major tryptic digestion product of the DNA-free enzyme arose from a cut next to a lysine (**Supplementary Fig. 6**).

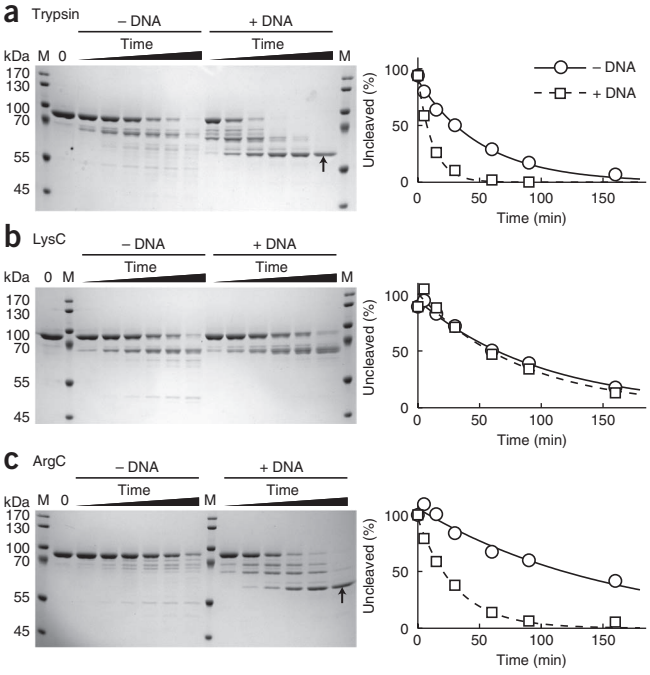

Figure 2 Limited proteolysis revealed a DNA-induced conformational change within the ATPase domain of ISWI. (**a–c**) Protease digestion of DNA-free and DNA-bound $ISWI_{26–648}$ by trypsin (**a**), LysC (**b**) and ArgC (**c**) for 5, 15, 30, 60, 90 and 160 min. Left, SDS-PAGE gels. Undigested protein served as the zero time point (0). M, molecular-weight marker. Right, quantification of the gel bands. The data were fit by a single exponential function (lines). Addition of 39-bp-long DNA duplexes (10 μM) led to a different banding pattern and 4.4-fold and 5.1-fold faster digestion rates by trypsin and ArgC, respectively, without affecting LysC digests. Arrows indicate a protease-stable fragment only seen in the presence of DNA.

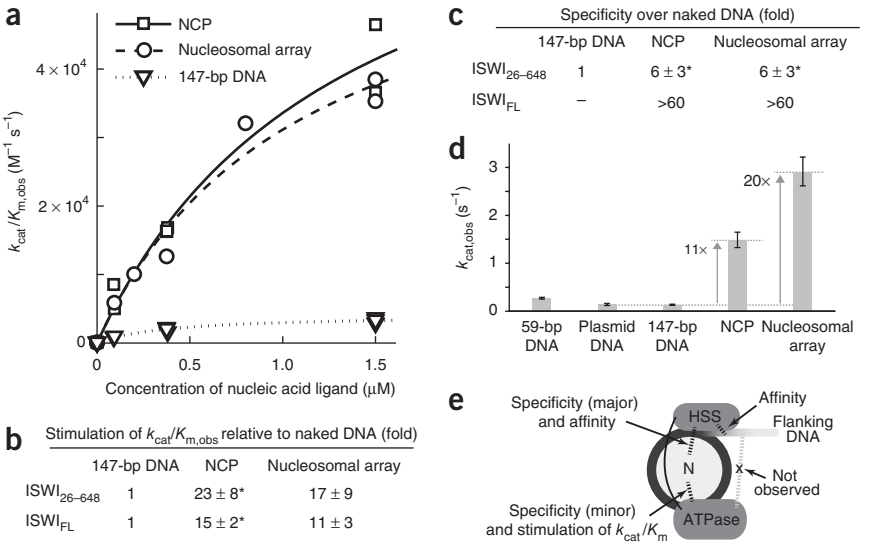

Figure 3 Interactions between domains of ISWI and the nucleosome and their importance for catalysis and substrate specificity. (**a**) Marked stimulation of $k_{cat}/K_{m,obs}$ for ATP hydrolysis of $ISWI_{26-648}$ (80 nM) by NCPs and nucleosomal arrays. Data were fit to a simple binding isotherm (lines). Results of two or more independent experiments are superimposed. (**b**) Stimulation of $k_{cat}/K_{m,obs}$ by NCPs and arrays relative to DNA. $k_{cat}/K_{m,obs}$ values for saturating concentrations of NCPs and arrays were normalized by corresponding values for 147-bp-long DNA (**Supplementary Table 1**). Where indicated (asterisks), errors are minimum and maximum values of two independent measurements. Otherwise, errors are s.d. ($n = 3$). (**c**) Discrimination between nucleosomal and naked DNA. $k_{cat}/K_{m,obs}$ values at subsaturating NCP and array concentrations were normalized by corresponding values for DNA-stimulated $ISWI_{26-648}$. Errors as in **b**. (**d**) Strong stimulation of $k_{cat,obs}$ of $ISWI_{FL}$ by saturating NCPs and arrays (200 nM enzyme; 0.5 mM ATP). Errors represent 95% confidence intervals of fits to a binding isotherm. (**e**) Summary of functional interactions (dashed lines) between ISWI and the nucleosome.

Notably, DNA binding did not affect the digestion kinetics of LysC, which provided strong evidence against occlusion (**Fig. 2b**). If accessibility of the lysine remained the same, then arginine residues must become more exposed with DNA to explain the trypsin results. We confirmed this prediction with the arginine-specific protease ArgC. ArgC produced a similar cleavage pattern as trypsin in the presence of DNA and experienced a similar rate enhancement by DNA (**Fig. 2a**,**c**). In summary, the proteolysis experiments showed that the enzyme conformation changed upon DNA binding. We suggest that these conformations are related to the conformations detected independently by the ATP-hydrolysis results above.

We noted that an ~60 kDa fragment accumulated in trypsin and ArgC digests when DNA was present (**Fig. 2a**,**c**), which suggested that DNA binding led to a well-folded, protease-resistant structure. N-terminal Edman sequencing and LC-MS/MS analysis of this fragment mapped the cleavage sites to accessory sequences outside of the ATPase core (Arg91 and Arg93 in the NTR and Arg589 at the C terminus; **Supplementary Fig. 3**). These accessory regions therefore took part in regulatory conformational changes induced by DNA binding (Discussion).

Nucleosome recognition involves the ATPase and HSS domains

Our data showed that the ISWI ATPase domain independently reacted to DNA association. We asked next whether the ATPase domain alone could specifically recognize an entire nucleosome, whether the HSS domain increased this specificity and to what extent stimulation of ATP hydrolysis by nucleosomes required the HSS domain.

We started by titrating nucleosomal arrays to $ISWI_{26-648}$ and $ISWI_{FL}$ under subsaturating ATP conditions, measuring the $k_{cat}/K_{m,obs}$ (**Fig. 3a**,**b**). Effects of nucleosomes on the affinity of ATP (discussed above) should be detectable under these conditions, whereas they are masked with saturating ATP. Much to our surprise, saturating concentrations of nucleosomal arrays stimulated $ISWI_{26-648}$ much more strongly than DNA (17-fold). The level of stimulation and even the absolute hydrolysis rates were comparable between $ISWI_{26-648}$ and $ISWI_{FL}$ (**Fig. 3b** and **Supplementary Table 1**). These results indicated that $ISWI_{FL}$ and $ISWI_{26-648}$ could form the same important contacts to the nucleosome that mediated the stimulation.

We next probed whether these contacts were to linker DNA by deleting the linker altogether, using nucleosome core particles (NCPs). NCPs stimulated hydrolysis of $ISWI_{26-648}$ just as well as arrays. Also the apparent affinity of arrays and NCPs remained unaffected (**Fig. 3a**). Notably, even $ISWI_{FL}$ did not react to deletion of the linker (**Fig. 3b**). These results ruled out that the contact responsible for ATPase stimulation was between the HSS domain and linker DNA.

When ATP and DNA ligand are subsaturating, the specificity with which ISWI discriminates between different DNA ligands can be determined (ref. 38 and mathematical derivation not shown). $ISWI_{26-648}$ possessed a moderate ability to distinguish between naked and nucleosomal DNA (six-fold for both NCPs and arrays). In contrast, $ISWI_{FL}$ strongly discriminated between naked and nucleosomal DNA (>60-fold for both NCPs and arrays; **Fig. 3c**). This result indicated that the HSS domain formed important contacts to the NCP, which increased the specificity for nucleosomes. Because of tight binding, we could only extract lower limits for the specificity of $ISWI_{FL}$. For the same reason, we could not test whether HSS-linker interactions provided additional specificity. In addition to specificity, the HSS domain markedly improved the apparent affinity for nucleosomes, as $ISWI_{FL}$ saturated with much lower concentrations of nucleosomes than $ISWI_{26-648}$ (≤25 nM versus >0.5 μM, respectively; **Fig. 3a** and data not shown).

We confirmed that the HSS–linker DNA interaction is also negligible for ATPase activation under saturating ATP conditions (**Fig. 3d**). NCPs stimulated the $k_{cat,obs}$ by 11-fold relative to naked DNA, whereas nucleosomal arrays stimulated $k_{cat,obs}$ at most by ~two-fold more than NCPs. Notably, $ISWI_{26-648}$ apparently lost its ability to discriminate free DNA from NCPs or arrays with saturating ATP, as all these ligands gave indistinguishable stimulation at similar concentrations (data not shown). This result suggested that the relatively poor discriminatory power that $ISWI_{26-648}$ possessed at subsaturating ATP concentrations was further reduced when the enzyme was saturated with nucleotides, which resulted in enzyme that did not profit from the nucleosomal activation at SHL2 (discussed below) but instead sampled DNA elsewhere on the surface of the nucleosome (**Supplementary Note**). **Figure 3e** summarizes ISWI-nucleosome interactions and their functions uncovered in this section.

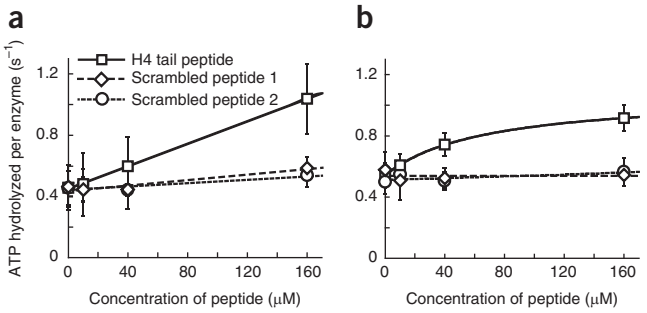

Figure 4 An N-terminal peptide of histone H4 activated ISWI ATP turnover. (**a**,**b**) ATP hydrolysis rates of $ISWI_{FL}$ (**a**) and $ISWI_{26–648}$ (**b**), both 0.5 μM, in the presence of DNA (1.2 mg ml^{-1} salmon sperm DNA) and saturating ATP concentrations (1 mM). Two peptides with a scrambled amino acid sequence served as specificity controls. Error bars, s.d. ($n = 4$).

The ATPase domain senses the histone H4 N-terminal tail

Stimulation of ATP turnover by nucleosomes has been shown to require the histone H4 N-terminal tail[17,19]. The location of the H4 tail near the interaction site of the ATPase domain at SHL2 would be consistent with a direct effect of the H4 tail on the ATPase domain. Structural similarity of the SANT domain with histone tail–binding proteins, however, would point to the HSS domain as the sensor of the H4 tail[23,39]. Using $ISWI_{26–648}$, we directly tested whether the HSS domain is required to detect the H4 tail.

In a previous publication, we showed that ATP turnover was faster when $ISWI_{FL}$ was presented with a synthetic H4 tail peptide in addition to DNA[40]. Surprisingly, $ISWI_{26–648}$ was similarly sensitive to the presence of the peptide (**Fig. 4**). On the basis of these results, we suggest that the HSS domain is not necessary for the recognition of the H4 tail, a conclusion that is further corroborated below.

The ATPase domain is sufficient to remodel nucleosomes

Our results so far argued that many important functionalities of ISWI are built into its ATPase module. We were curious as to whether these functionalities also sufficed to remodel nucleosomes, which would be consistent with recent evidence obtained for Chd1 (refs. 11,31), or whether additional conformational changes between the HSS and ATPase were required for remodeling, as previously suggested[2,3,24,30].

We analyzed nucleosome remodeling in three different ways. First, we probed whether $ISWI_{26–648}$ could reposition the histone octamer in mononucleosomes, an activity that is well documented for $ISWI_{FL}$[41]. Differently positioned nucleosomes can be visualized through their different mobility in native gels. Unexpectedly, the reaction products generated by $ISWI_{26–648}$ in this assay resembled those of $ISWI_{FL}$ (**Fig. 5a**).

Second, we tested nucleosome repositioning in the context of 25-mer nucleosomal arrays, a more physiological substrate (**Fig. 5b**). Each linker DNA contained an exposed AvaI restriction site. As expected, AvaI fully digested unremodeled arrays to mononucleosomes. After remodeling by $ISWI_{26–648}$, in contrast, AvaI could not fully digest the arrays, which indicated occlusion of a fraction of AvaI sites by nucleosomes (**Fig. 5c**). Protection of these sites by binding of ISWI was ruled out by experiments that lacked ATP and by exhaustive AvaI digests.

The third assay probed accessibility of restriction sites that were protected by nucleosomes in the array before remodeling[42]. Accessibility of four restriction enzyme sites, distributed over an entire gyre of nucleosomal DNA, dramatically changed upon incubation with $ISWI_{26–648}$ in an ATP hydrolysis–dependent manner (**Fig. 5d**).

To quantify the effect of the deletion of the HSS domain on remodeling, we adapted a previously described assay[43]. We generated nucleosomal arrays in which the central nucleosome protected a unique restriction site before remodeling (KpnI; **Fig. 6a**). By following the accessibility of the KpnI site, we collected time courses for increasing ISWI concentrations at saturating ATP and plotted the observed remodeling rate constants over the enzyme concentration to obtain the maximal reaction velocity (**Fig. 6b–d** and **Supplementary Fig. 7**). Comparison of the maximal velocities showed that $ISWI_{FL}$ remodeled arrays approximately an order of magnitude faster than $ISWI_{26–648}$ (**Fig. 6e**). As shown above, $ISWI_{FL}$ also hydrolyzed ATP at an order of magnitude faster than $ISWI_{26–648}$ under similar conditions, owing to improved binding specificity. Thus, per ATP hydrolyzed, the efficiency of remodeling was similar for both enzymes.

Deletion of the histone H4 tail was shown to impair remodeling by $ISWI_{FL}$[15–19]. Remodeling by $ISWI_{26–648}$ should be similarly affected if, as we suggested above, the ATPase domain directly recognized the H4 tail. By monitoring remodeling of nucleosomal arrays that lacked the H4 N-terminal tail, we found that $ISWI_{26–648}$ was at least

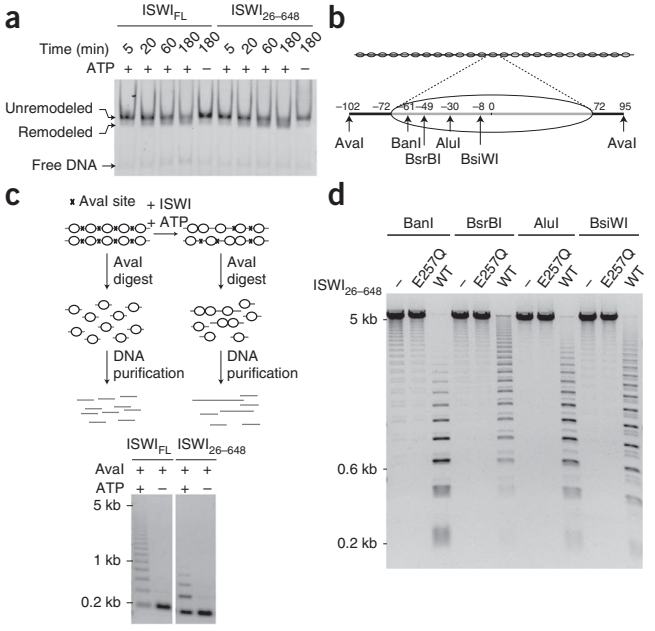

Figure 5 The HSS domain is not required for repositioning mononucleosomes or nucleosomes within arrays. (**a**) Mononucleosome-sliding assay. Mononucleosomes, centrally positioned on a 197-bp Widom-601 DNA, were incubated for the indicated time with ATP and ISWI and analyzed by native PAGE. Quench DNA migrated more slowly and was cut off for clarity. Control reactions (–) were depleted of ATP with apyrase before addition of ISWI. (**b**) Schematic depiction of the 25-mer nucleosomal arrays used in **c** and **d**. Each nucleosome protected the indicated restriction enzyme sites, whereas the linker DNA contained an exposed AvaI site (magnification). Numbers specify base pairs relative to the pseudodyad axis (0). (**c**) Polynucleosome-sliding assay. Top, schematic depiction of the assay. Bottom, nucleosomal arrays incubated with ISWI and ATP as indicated. Control reactions were depleted of ATP as above (–). kb, kilobases. (**d**) Restriction enzyme accessibility assays. Nucleosomal arrays were incubated with ATP, the indicated restriction enzymes and wild-type (WT) or mutant $ISWI_{26–648}$ (E257Q). DNA was then deproteinized and resolved by gel electrophoresis. Samples incubated without enzyme (–) served as controls.

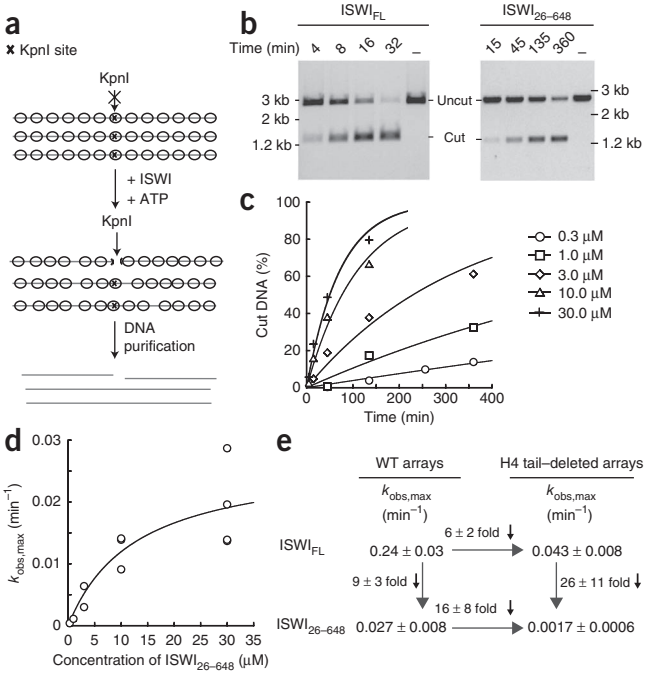

Figure 6 Remodeling by ISWI$_{26–648}$ is only moderately slower than remodeling by ISWI$_{FL}$, and it is sensitive to H4 tail deletion. (**a**) Schematic depiction of the remodeling assay. The central nucleosome in a 13-mer nucleosomal array occluded a unique KpnI site. (**b**) Exemplary time courses for remodeling by ISWI$_{FL}$ and ISWI$_{26–648}$ (both 3 μM). In control reactions (–), the quench solution was added together with ATP. (**c**) Time-course data collected for varying ISWI$_{26–648}$ concentrations and fit to a single exponential function to extract the rate constant k_{obs} (line). (**d**) Maximal velocity with which ISWI$_{26–648}$ remodeled nucleosomes ($k_{obs,max}$), obtained by extrapolating to saturating enzyme concentrations (lines). Data points were from several independent experiments. (**e**) Effects of HSS and H4 tail deletion on the maximal remodeling velocities $k_{obs,max}$. Values for $k_{obs,max}$ for ISWI$_{FL}$ and ISWI$_{26–648}$ were obtained as above at saturating ATP concentrations (**Supplementary Fig. 7**). Errors are standard errors of the fit.

as sensitive toward deletion of the H4 tail as ISWI$_{FL}$, confirming our previous conclusion (16-fold; **Fig. 6e**).

DISCUSSION

Our major conclusion is that—contrary to widespread belief—all fundamental aspects of nucleosome-remodeling catalysis are contained within the compact ATPase domain of ISWI. The ATPase module alone was able to recognize the DNA and histone moiety of substrate nucleosomes. Substrate binding triggered a conformational change within the ATPase domain along with an increased affinity for ATP. The ATPase module alone was able to remodel nucleosomes. In conjunction with recent related observations for the Chd1 remodeler[11], these findings suggest that nucleosome remodeling could have evolved from helicase-type motors without further requirements for accessory domains[44].

Mechanistic implications for nucleosome remodeling

Several current models ascribe critical functions to the HSS domain during remodeling. The HSS domain was suggested to bind and release DNA and drag it into the nucleosome upon cues from the ATPase domain, to form channels for nucleosomal DNA or to stabilize high-energy structures such as DNA bulges off the histone surface[2–4,16,24,30]. Notably, we found that ISWI lacking its HSS domain still remodeled nucleosomes, although the reaction proceeded an order of magnitude more slowly. This defect, however, was accounted for by a proportionally decreased ATP turnover. We therefore conclude that the HSS domain is not an integral component of the motor core of ISWI.

Whereas passive secondary roles of the HSS during remodeling are fully consistent with our results (discussed below), our ATPase data do not favor models that postulate active coordination, that is, transduction of energy, between the ATPase and the HSS domains. Steady-state ATP hydrolysis parameters ($k_{cat}/K_{m,obs}$) of ligand-free, DNA-bound and nucleosome-bound ISWI largely remained unaffected when the HSS was deleted. Notably, the characteristic biphasic ATP concentration dependence of hydrolysis was preserved when the HSS domain was missing. It remains possible, though, that energy is transduced only after the rate-limiting step of ATP hydrolysis, because steady-state measurements are blind to that regime.

The autonomy of the ATPase domain does not appear to be a specialty of ISWI, because Chd1 derivatives that lack their C-terminal DNA-binding domain can still slide nucleosomes[11,31]. This commonality adds to the growing list of shared functional properties of ISWI and Chd1 remodelers (ref. 28 and references therein). In fact, substantial parts of both enzymes are also structurally related. Chd1 harbors a SANT-SLIDE domain in place of the HSS domain of ISWI[28], and both enzymes contain the bridge motif adjacent to the conserved ATPase domain[31,32]. Although the N-terminal parts of both enzymes lack any apparent homology, they nevertheless may perform similar functions (discussed below).

How does ISWI remodel nucleosomes without the involvement of the HSS domain? Previous studies placed the ATPase region of several remodelers close to SHL2 of the nucleosome, whereas the HSS domain of ISWI was found to bind the linker DNA[9–11,18,24,25,45]. As ISWI$_{26–648}$ discriminates between nucleosomes and DNA and is sensitive to the H4 tail, at least a fraction of ISWI$_{26–648}$ can productively bind at SHL2 (**Fig. 7a**, step 1).

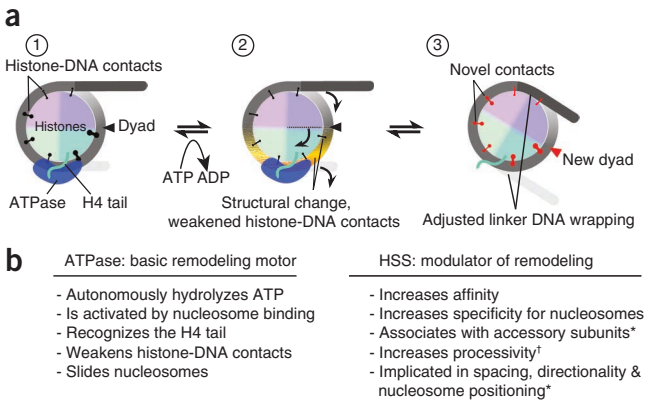

Figure 7 Model for the mechanism of nucleosome remodeling. (**a**) Suggested remodeling mechanism. The HSS domain was omitted from the model, as it is not required for the basic mechanism. Histones and DNA form multiple contacts of varying strength (black clamps; shown only for the top gyre of DNA). The ATPase domain attaches to histones, for example the H4 N terminus (1). Upon ATP hydrolysis, the ATPase domain translocates DNA relative to the histones, thereby distorting the nucleosome structure and disrupting DNA-histone interactions in the vicinity of SHL2 (2). With the strongest histone-DNA contacts destabilized, the histones rearrange relative to DNA to optimize interactions, forming a new set of contacts and thus a repositioned nucleosome (red clamps; 3). (**b**) Division of labor between the ATPase and HSS domains. Asterisks indicate prior work; dagger, anticipated function.

Strong histone-DNA contacts are present around SHL2 (refs. 46,47). Weakening the strongest contacts is expected to be rate limiting for remodeling. This could occur when the binding energy of the remodeler toward the nucleosome is exploited[48] or when the ATPase domain tries to translocate on DNA while interacting with histones, for example, at the H4 tail. Translocation puts a strain on the nucleosome, caused either by the presence of excess DNA or by a change in the twist of the DNA, which locally destabilizes histone-DNA interactions (**Fig. 7a**, step 2)[12,13,22]. The ATPase domain may even be strong enough to pump more DNA toward the dyad than the nucleosomal surface can accommodate, causing it to detach and bulge out[2,16,18,30,49]. The latter model is difficult to envision for remodeling by the truncated ISWI enzyme, owing to a lack of domains that help form and stabilize the bulge.

Once key contacts between histones and DNA are weakened, alternative sets of histone-DNA contacts might become energetically more preferable, leading to a repositioning of the histones relative to DNA (**Fig. 7a**, step 3). DNA-histone contacts may adjust concertedly or—perhaps more probably—only locally, such that the strain propagates in multiple steps around the nucleosome[4,22].

Accessory domains may have evolved to optimize catalysis and modulate the outcome of the reaction, which explains their diversity among remodeling machines (**Fig. 7b**)[2,4]. We showed that, consistent with previous findings[23], the HSS domain increased the affinity of ISWI toward DNA, a feature that is expected to enhance processivity[16,50,51]. In agreement with cross-linking results[24], we obtained evidence for direct contacts between the HSS domain and the NCP. This interaction was a major source for specificity toward the nucleosome. As such, the HSS domain improves the productive association of the ATPase domain at SHL2, which in turn enhances remodeling. The HSS domain could also optimize catalysis by weakening the DNA-histone interactions at the edge of the nucleosome[11,16]. Through interactions with additional subunits and the linker DNA[23–25,36,52], the HSS may assist sensing the length of the linker or a preferred DNA sequence and therefore bias the remodeling reaction toward specific outcomes such as nucleosome spacing or positioning[11,24,25,27,28].

Conformational changes within the ATPase domain

How do the conformational changes within the ATPase domain relate to previously reported structural changes in related enzymes? The catalytic domain of the distant relative *Sulfolobus* Sso1653 was crystallized with and without bound DNA[35]. The two structures showed only minor differences well inside the ATPase core and therefore are unlikely to account for the increased exposure of peripheral arginines upon DNA binding. In conflict with the crystallographic data but in better agreement with our results, a FRET study using the same *Sulfolobus* protein concluded that DNA binding leads to a major structural rearrangement between the two ATPase lobes[37].

Additional crystallographic evidence supports a high degree of flexibility between the two ATPase lobes. The ATPase lobes of relatives of ISWI crystallized in a multitude of very different orientations[31,35,53,54]. Conformational changes between the two ATPase lobes may be functionally important for these enzymes, for example, for translocation on DNA or regulation of enzyme activity[5,44]. Conceivably, multiple orientations of ISWI's ATPase lobes coexist in solution, accounting for the different enzyme species detected by our ATPase experiments[32]. DNA may preferentially stabilize a subset of these states, thereby aligning the composite catalytic site formed at the cleft between both lobes[5]. As motifs of both ATPase lobes are thought to contact ATP[35], a proper alignment of the lobes might increase the affinity for ATP, explaining our biochemical data.

The increased exposure of peripheral arginines upon DNA binding also suggests that these regions undergo structural changes. Trypsin cleaved DNA-bound ISWI adjacent to a conserved acidic motif in the NTR (**Supplementary Fig. 3**). Despite a lack of sequence similarity, the NTR of Chd1 also contains a highly acidic motif, which was suggested to act as a pseudosubstrate and compete with DNA for binding to lobe 2. The authors proposed that, in excellent agreement with our proteolytic results, DNA binding would force a structural rearrangement in Chd1 in which the NTR undocks from lobe 2 (ref. 31). The NTRs of both enzymes may therefore fulfill similar roles and gate the entrance to the nucleic acid–binding site.

On the C-terminal side, trypsin cut the polypeptide chain within the 'brace' motif of lobe 2 (ref. 4). The brace is in close contact with lobe 1 and is directly followed by a stretch of amino acids that folds back to form a bridge between both ATPase lobes[31,32]. We suggest that the brace or bridge may hold the ATPase lobes in a configuration that is not fully competent for ATP hydrolysis and that binding of nucleic acids relieves this inhibition. These results reinforce the notion that the ATPase domain represents an autonomous remodeling engine, which is optimized and modulated by the evolution of accessory domains and subunits.

METHODS

Methods and any associated references are available in the online version of the paper.

Note: Supplementary information is available in the online version of the paper.

ACKNOWLEDGMENTS

We are grateful to C. Müller (European Molecular Biology Laboratory, Heidelberg, Germany) and D. Rhodes (Nanyang Technological University, Singapore) for the donation of plasmids and to the following colleagues at Ludwig-Maximilians-Universität, Munich, Germany, for materials: N. Hepp for 13-mer nucleosomal arrays, C. Boenisch for 197-bp 601 DNA, V.K. Maier and C. Regnard for recombinant histone octamers. We thank R. Mentele for the Edman digest, I. Forné for performing the LC-MS/MS experiment and Z. Ökten for comments on the manuscript. H.K. acknowledges support by the Elite Network of Bavaria. This work was supported by grants of the Deutsche Forschungsgemeinschaft to P.B.B. (SFB 594 TP A6 and Be 1140/6-1).

AUTHOR CONTRIBUTIONS

F.M.-P., H.K. and J.L. performed experiments. All authors interpreted results and contributed to writing.

COMPETING FINANCIAL INTERESTS

The authors declare no competing financial interests.

Published online at http://www.nature.com/doifinder/10.1038/nsmb.2457.
Reprints and permissions information is available online at http://www.nature.com/reprints/index.html.

1. Hargreaves, D.C. & Crabtree, G.R. ATP-dependent chromatin remodeling: genetics, genomics and mechanisms. *Cell Res.* **21**, 396–420 (2011).
2. Clapier, C.R. & Cairns, B.R. The biology of chromatin remodeling complexes. *Annu. Rev. Biochem.* **78**, 273–304 (2009).
3. Hota, S.K. & Bartholomew, B. Diversity of operation in ATP-dependent chromatin remodelers. *Biochim. Biophys. Acta* **1809**, 476–487 (2011).
4. Flaus, A. & Owen-Hughes, T. Mechanisms for ATP-dependent chromatin remodelling: the means to the end. *FEBS J.* **278**, 3579–3595 (2011).
5. Hauk, G. & Bowman, G.D. Structural insights into regulation and action of SWI2/SNF2 ATPases. *Curr. Opin. Struct. Biol.* **21**, 719–727 (2011).
6. Flaus, A., Martin, D.M., Barton, G.J. & Owen-Hughes, T. Identification of multiple distinct Snf2 subfamilies with conserved structural motifs. *Nucleic Acids Res.* **34**, 2887–2905 (2006).
7. Dechassa, M.L. *et al.* Disparity in the DNA translocase domains of SWI/SNF and ISW2. *Nucleic Acids Res.* 4412–4421 (2012).
8. Fan, H.Y., Trotter, K.W., Archer, T.K. & Kingston, R.E. Swapping function of two chromatin remodeling complexes. *Mol. Cell* **17**, 805–815 (2005).
9. Saha, A., Wittmeyer, J. & Cairns, B.R. Chromatin remodeling through directional DNA translocation from an internal nucleosomal site. *Nat. Struct. Mol. Biol.* **12**, 747–755 (2005).

10. Zofall, M., Persinger, J., Kassabov, S.R. & Bartholomew, B. Chromatin remodeling by ISW2 and SWI/SNF requires DNA translocation inside the nucleosome. *Nat. Struct. Mol. Biol.* **13**, 339–346 (2006).
11. McKnight, J.N., Jenkins, K.R., Nodelman, I.M., Escobar, T. & Bowman, G.D. Extranucleosomal DNA binding directs nucleosome sliding by Chd1. *Mol. Cell. Biol.* **31**, 4746–4759 (2011).
12. Richmond, T.J. & Davey, C.A. The structure of DNA in the nucleosome core. *Nature* **423**, 145–150 (2003).
13. Suto, R.K. *et al.* Crystal structures of nucleosome core particles in complex with minor groove DNA-binding ligands. *J. Mol. Biol.* **326**, 371–380 (2003).
14. Makde, R.D., England, J.R., Yennawar, H.P. & Tan, S. Structure of RCC1 chromatin factor bound to the nucleosome core particle. *Nature* **467**, 562–566 (2010).
15. Ferreira, H., Flaus, A. & Owen-Hughes, T. Histone modifications influence the action of Snf2 family remodelling enzymes by different mechanisms. *J. Mol. Biol.* **374**, 563–579 (2007).
16. Gangaraju, V.K., Prasad, P., Srour, A., Kagalwala, M.N. & Bartholomew, B. Conformational changes associated with template commitment in ATP-dependent chromatin remodeling by ISW2. *Mol. Cell* **35**, 58–69 (2009).
17. Clapier, C.R., Langst, G., Corona, D.F., Becker, P.B. & Nightingale, K.P. Critical role for the histone H4 N terminus in nucleosome remodeling by ISWI. *Mol. Cell. Biol.* **21**, 875–883 (2001).
18. Dang, W., Kagalwala, M.N. & Bartholomew, B. Regulation of ISW2 by concerted action of histone H4 tail and extranucleosomal DNA. *Mol. Cell. Biol.* **26**, 7388–7396 (2006).
19. Hamiche, A., Kang, J.G., Dennis, C., Xiao, H. & Wu, C. Histone tails modulate nucleosome mobility and regulate ATP-dependent nucleosome sliding by NURF. *Proc. Natl. Acad. Sci. USA* **98**, 14316–14321 (2001).
20. Whitehouse, I., Stockdale, C., Flaus, A., Szczelkun, M.D. & Owen-Hughes, T. Evidence for DNA translocation by the ISWI chromatin-remodeling enzyme. *Mol. Cell. Biol.* **23**, 1935–1945 (2003).
21. Zhang, Y. *et al.* DNA translocation and loop formation mechanism of chromatin remodeling by SWI/SNF and RSC. *Mol. Cell* **24**, 559–568 (2006).
22. Bowman, G.D. Mechanisms of ATP-dependent nucleosome sliding. *Curr. Opin. Struct. Biol.* **20**, 73–81 (2010).
23. Grüne, T. *et al.* Crystal structure and functional analysis of a nucleosome recognition module of the remodeling factor ISWI. *Mol. Cell* **12**, 449–460 (2003).
24. Dang, W. & Bartholomew, B. Domain architecture of the catalytic subunit in the ISW2-nucleosome complex. *Mol. Cell. Biol.* **27**, 8306–8317 (2007).
25. Yamada, K. *et al.* Structure and mechanism of the chromatin remodelling factor ISW1a. *Nature* **472**, 448–453 (2011).
26. Gangaraju, V.K. & Bartholomew, B. Dependency of ISW1a chromatin remodeling on extranucleosomal DNA. *Mol. Cell. Biol.* **27**, 3217–3225 (2007).
27. Yang, J.G., Madrid, T.S., Sevastopoulos, E. & Narlikar, G.J. The chromatin-remodeling enzyme ACF is an ATP-dependent DNA length sensor that regulates nucleosome spacing. *Nat. Struct. Mol. Biol.* **13**, 1078–1083 (2006).
28. Ryan, D.P., Sundaramoorthy, R., Martin, D., Singh, V. & Owen-Hughes, T. The DNA-binding domain of the Chd1 chromatin-remodelling enzyme contains SANT and SLIDE domains. *EMBO J.* **30**, 2596–2609 (2011).
29. Corona, D.F. *et al.* ISWI is an ATP-dependent nucleosome remodeling factor. *Mol. Cell* **3**, 239–245 (1999).
30. Cairns, B.R. Chromatin remodeling: insights and intrigue from single-molecule studies. *Nat. Struct. Mol. Biol.* **14**, 989–996 (2007).
31. Hauk, G., McKnight, J.N., Nodelman, I.M. & Bowman, G.D. The chromodomains of the Chd1 chromatin remodeler regulate DNA access to the ATPase motor. *Mol. Cell* **39**, 711–723 (2010).
32. Forne, I., Ludwigsen, J., Imhof, A., Becker, P.B. & Mueller-Planitz, F. Probing the conformation of the ISWI ATPase domain with genetically encoded photoreactive crosslinkers and mass spectrometry. *Mol Cell Proteomics* **11**, M111.012088 (2012).
33. Racki, L.R. *et al.* The chromatin remodeller ACF acts as a dimeric motor to space nucleosomes. *Nature* **462**, 1016–1021 (2009).
34. Singleton, M.R., Dillingham, M.S. & Wigley, D.B. Structure and mechanism of helicases and nucleic acid translocases. *Annu. Rev. Biochem.* **76**, 23–50 (2007).
35. Dürr, H., Korner, C., Muller, M., Hickmann, V. & Hopfner, K.P. X-ray structures of the *Sulfolobus solfataricus* SWI2/SNF2 ATPase core and its complex with DNA. *Cell* **121**, 363–373 (2005).
36. Sharma, A., Jenkins, K.R., Heroux, A. & Bowman, G.D. Crystal structure of the chromodomain helicase DNA-binding protein 1 (Chd1) DNA-binding domain in complex with DNA. *J. Biol. Chem.* **286**, 42099–42104 (2011).
37. Lewis, R., Durr, H., Hopfner, K.P. & Michaelis, J. Conformational changes of a Swi2/Snf2 ATPase during its mechano-chemical cycle. *Nucleic Acids Res.* **36**, 1881–1890 (2008).
38. Fersht, A. *Structure and Mechanism in Protein Science: A Guide to Enzyme Catalysis and Protein Folding* (W.H. Freeman, 1999).
39. Boyer, L.A., Latek, R.R. & Peterson, C.L. The SANT domain: a unique histone-tail-binding module? *Nat. Rev. Mol. Cell Biol.* **5**, 158–163 (2004).
40. Clapier, C.R., Nightingale, K.P. & Becker, P.B. A critical epitope for substrate recognition by the nucleosome remodeling ATPase ISWI. *Nucleic Acids Res.* **30**, 649–655 (2002).
41. Längst, G., Bonte, E.J., Corona, D.F. & Becker, P.B. Nucleosome movement by CHRAC and ISWI without disruption or trans-displacement of the histone octamer. *Cell* **97**, 843–852 (1999).
42. Maier, V.K., Chioda, M., Rhodes, D. & Becker, P.B. ACF catalyses chromatosome movements in chromatin fibres. *EMBO J.* **27**, 817–826 (2008).
43. Logie, C. & Peterson, C.L. Catalytic activity of the yeast SWI/SNF complex on reconstituted nucleosome arrays. *EMBO J.* **16**, 6772–6782 (1997).
44. Dürr, H., Flaus, A., Owen-Hughes, T. & Hopfner, K.P. Snf2 family ATPases and DExx box helicases: differences and unifying concepts from high-resolution crystal structures. *Nucleic Acids Res.* **34**, 4160–4167 (2006).
45. Kagalwala, M.N., Glaus, B.J., Dang, W., Zofall, M. & Bartholomew, B. Topography of the ISW2-nucleosome complex: insights into nucleosome spacing and chromatin remodeling. *EMBO J.* **23**, 2092–2104 (2004).
46. Hall, M.A. *et al.* High-resolution dynamic mapping of histone-DNA interactions in a nucleosome. *Nat. Struct. Mol. Biol.* **16**, 124–129 (2009).
47. Mihardja, S., Spakowitz, A.J., Zhang, Y. & Bustamante, C. Effect of force on mononucleosomal dynamics. *Proc. Natl. Acad. Sci. USA* **103**, 15871–15876 (2006).
48. Lorch, Y., Maier-Davis, B. & Kornberg, R.D. Mechanism of chromatin remodeling. *Proc. Natl. Acad. Sci. USA* **107**, 3458–3462 (2010).
49. Strohner, R. *et al.* A 'loop recapture' mechanism for ACF-dependent nucleosome remodeling. *Nat. Struct. Mol. Biol.* **12**, 683–690 (2005).
50. Blosser, T.R., Yang, J.G., Stone, M.D., Narlikar, G.J. & Zhuang, X. Dynamics of nucleosome remodelling by individual ACF complexes. *Nature* **462**, 1022–1027 (2009).
51. Fyodorov, D.V. & Kadonaga, J.T. Dynamics of ATP-dependent chromatin assembly by ACF. *Nature* **418**, 897–900 (2002).
52. Eberharter, A., Vetter, I., Ferreira, R. & Becker, P.B. ACF1 improves the effectiveness of nucleosome mobilization by ISWI through PHD-histone contacts. *EMBO J.* **23**, 4029–4039 (2004).
53. Thomä, N.H. *et al.* Structure of the SWI2/SNF2 chromatin-remodeling domain of eukaryotic Rad54. *Nat. Struct. Mol. Biol.* **12**, 350–356 (2005).
54. Caruthers, J.M., Johnson, E.R. & McKay, D.B. Crystal structure of yeast initiation factor 4A, a DEAD-box RNA helicase. *Proc. Natl. Acad. Sci. USA* **97**, 13080–13085 (2000).

ONLINE METHODS

Enzyme expression and purification. pPROEX-HTb–based expression plasmids with genes encoding *Drosophila* $ISWI_{FL}$, $ISWI_{FL}$ E257Q, $ISWI_{26–648}$ and $ISWI_{1–697}$ were kindly provided by C. Müller (EMBL, Heidelberg, Germany). All genes were fused N terminally to a His_6-TEV tag . The E257Q mutation was introduced into $ISWI_{26–648}$ by QuikChange mutagenesis (Stratagene). Expression and purification was performed as described[32]. The His_6-TEV tag was cleaved off by TEV protease for $ISWI_{FL}$ and $ISWI_{1–697}$. For $ISWI_{26–648}$, experiments were carried out in the presence of the tag. ATPase parameters of $ISWI_{26–648}$ with and without tag were quantitatively the same (data not shown).

Enzyme assays and enzyme ligands. Unless otherwise stated, reactions were performed at 28 °C in a buffer containing 25 mM HEPES-KOH, pH 7.6, 100 mM potassium acetate, 1.5 mM magnesium acetate, 0.1 mM EDTA, 10% glycerol, 10 mM β-mercaptoethanol. As indicated, some ATPase assays were performed in a buffer with an increased buffering capacity (250 mM HEPES-KOH, pH 7.6) and excess Mg^{2+} ions (100 mM magnesium acetate) to prevent high concentrations of ATP from substantially altering the pH and the concentration of free unchelated Mg^{2+} ions. Both buffers yielded comparable ATPase parameters (**Table 1** and **Supplementary Table 1**). Remodeling was followed in 25 mM HEPES-KOH, pH 7.6, 50 mM NaCl, 1 mM MgCl, 0.1 mM EDTA, 10% glycerol and 1 mM DTT at 26 °C. All remodeling reactions contained an ATP-regenerating system consisting of phosphoenolpyruvate (3–6 mM) and a pyruvate kinase-lactate dehydrogenase mixture (15.5 U/ml; Sigma). Nucleotides were always added as stoichiometric complexes with Mg^{2+}. ADP and AMPPNP were purified before use[55]. ATP was purified if used at concentrations exceeding 3 mM or if no ATP regenerating system was used.

HPLC-purified oligopeptides and DNA oligonucleotides were purchased (Peptide Specialty Laboratories and Biomers, respectively; **Supplementary Table 2**). Short DNA duplexes were created by annealing. The 147-bp DNA used for NCP reconstitution was purified from SmaI digests of a plasmid harboring derivatives of the Widom-601 sequence with terminal SmaI sites. 197-bp DNA was generated by AvaI digests of a pUC derivative containing 25 repeats of the Widom-601 sequence (kindly provided by D. Rhodes, NTU, Singapore). During nucleosome assembly, it is expected that the 147-bp and 197-bp DNA form 0-N-2 and 29-N-23 nucleosomes, respectively[14,56]. DNA used for 13-mer nucleosomal arrays was gene synthesized (Genscript). It contained 197-bp repeats of Widom-601 derivatives with a KpnI site at position −32 relative to the dyad axis of the central nucleosome.

Mono- and polynucleosomes were reconstituted with recombinant *Drosophila* histones by salt-gradient dialysis as described[57,58]. H4 tail–deleted arrays lacked the 19 N-terminal amino acids of histone H4. Nucleosomal arrays were purified by Mg^{2+} precipitation (25-mer arrays, 3.5 mM; 13-mer WT-H4 arrays, 5 mM; 13-mer H4 tail–deleted arrays, 8.5 mM)[42,58]. The 13-mer arrays were subsequently dialyzed into 10 mM Tris, pH 7.7, 0.1 mM EDTA, pH 8, 1 mM DTT. Mononucleosomes used in the TLC ATPase assay were purified over a glycerol gradient (10% to 30%) and buffer exchanged into reaction buffer by ultrafiltration. The concentration of nucleosomal DNA was determined by measuring its DNA content by UV absorbance at 260 nm. The indicated concentrations of nucleosomal arrays refer to the concentration of individual nucleosomes. Unless otherwise noted, nucleosomes with WT-H4 were used.

Steady-state ATP hydrolysis assays. Two different ATPase assays were employed. A thin-layer chromatography (TLC)–based assay was used to follow hydrolysis of [γ-^{32}P]ATP in reactions that required the use of subsaturating ATP concentrations (**Fig. 3a–c** and **Supplementary Fig. 4**). All other ATPase data were collected by a coupled ATP-hydrolysis assay in 384-well plates as described[32]. For the TLC assay, reactions were initiated by addition of trace amounts of [γ-^{32}P]ATP supplemented with 1 μm purified, nonradioactive ATP. Three time points (in addition to a 'zero' time point from a reaction that lacked enzyme) were collected by stopping the reaction with three volumes of 2 mM EDTA, 0.3 M NaH_2PO_4, 1 M LiCl. Control experiments showed that ISWI was fully quenched on time scales that were much faster than the experiments required. Reactions were spotted on PEI cellulose F (Merck) and developed in 0.3 M NaH_2PO_4, 1 M LiCl. After autoradiography, signals were quantified, and a line was fit through the data points of each time course. $k_{cat}/K_{m,obs}$ values were obtained from the slopes by normalizing for the enzyme concentration. When the enzyme and ATP concentrations were varied four- and five-fold, respectively, measured rates deviated less than two-fold.

Partial proteolysis assays. If not specified otherwise, $ISWI_{26–648}$ (2.5 μM) was partially proteolyzed with trypsin (20 nM; Promega), LysC (38 nM; Roche) or ArgC (21 nM; Roche). The reaction was stopped by addition of two volumes of SDS sample buffer and immediate incubation at 95 °C for 10 min. Samples were separated by SDS-PAGE (12%) and stained by Coomassie Blue.

Double-filter DNA-binding assay. 39-bp DNA was 5′ labeled with [γ-^{32}P]ATP by polynucleotide kinase. Trace amounts of labeled DNA were incubated for 10 min with varying ISWI concentrations. The mixture was then applied on a membrane sandwich composed of a protein-binding (Protran-BA85, Whatman) and a DNA-binding membrane (Hybond-N+, Amersham) as described[59].

Nucleosome-sliding assays. For mononucleosome sliding, centrally positioned mononucleosomes (197-bp DNA; 160 nM) were incubated with ATP (0.5 mM), $ISWI_{FL}$ (30 nM) or $ISWI_{26–648}$ (300 nM). Time points were quenched by apyrase (2.5 U/μl) and excess linearized plasmid DNA (0.4 mg/ml). Native PAGE (4.5%) was performed with 0.2 μg mononucleosomal DNA.

For polynucleosome sliding, 25-mer regular nucleosomal arrays (30 nM) were incubated with ATP (100 μM) and $ISWI_{FL}$ (10 nM) or $ISWI_{26–648}$ (300 nM). Remodeling was quenched after 6 h with apyrase (2.5 U/μl). The arrays were then digested with AvaI (1.2 U/μl) for 3 h at 26 °C. Samples were deproteinized and analyzed as described below. Exhaustive digests with high concentrations of AvaI overnight gave analogous results.

Restriction enzyme accessibility assay. 25-mer nucleosomal arrays (100 nM) were incubated for 1 h with wild-type or E257Q mutant $ISWI_{26–648}$ (both 5 μM), ATP (50 μM) and the indicated restriction enzymes (AluI, 0.5 U/μl; BsrBI, 0.5 U/μl; BsiWI, 1 U/μl; BanI, 2 U/μl). The reactions were stopped with EDTA (20–40 mM) and SDS (0.4%). Samples were deproteinized, and DNA was ethanol precipitated, resolved by agarose gel electrophoresis and visualized by ethidium bromide staining.

To quantitate remodeling, 13-mer arrays (20 or 100 nM) were incubated with $ISWI_{FL}$ or $ISWI_{26–648}$, respectively, ATP (1 mM) and KpnI (2 U/μl). Reactions were quenched and analyzed as above. Negligible accessibility (<5%) was seen when the reaction was simultaneously initiated and quenched or when ISWI was omitted. Controls showed that the ATP-regenerating system was not depleted throughout the assay. k_{obs} for remodeling was obtained by fitting the time courses to a single exponential function (equation (1)). The maximal remodeling velocities ($k_{obs,max}$) were obtained by fitting the data to standard or inverse binding isotherms (equation (2)).

$$y = 100 * (1 - e^{-k_{obs} * t}) \quad (1)$$

$$y = k_{obs,max} - \left(amp * \frac{[E]}{K_{1/2} + [E]} \right) \quad (2)$$

Observed remodeling rates were proportionally faster for $ISWI_{26–648}$ (but not $ISWI_{FL}$) when the KpnI concentration was raised from 2 U/μl to 5 U/μl. This rate enhancement was independent of the $ISWI_{26–648}$ concentration between 0.3 and 30 μM. Reported rates, including the maximal remodeling rate constant $k_{obs,max,}$ are therefore lower estimates for $ISWI_{26–648}$. The reported deleterious effect of the HSS deletion on remodeling is consequently an upper estimate.

Kinetic and thermodynamic modeling and data fitting. Modeling was performed in Mathematica (Wolfram Research). Data were fit with Matlab (The Mathworks) or KaleidaGraph (Synergy Software). The biphasic ATPase data were fit to equation (3) (**Fig. 1a**,**b**). As saturation with ATP was not achieved, the second phase was represented only by the linear term m*[ATP]. m possesses a complex dependence on the rate and equilibrium constants in the reaction scheme (**Supplementary Fig. 1a**) and was not interpreted further.

$$v = k_{cat,obs,Phase\ 1} * [ATP] / (K_{m,obs,Phase\ 1} + [ATP]) + m * [ATP] \quad (3)$$

55. Horst, M., Oppliger, W., Feifel, B., Schatz, G. & Glick, B.S. The mitochondrial protein import motor: dissociation of mitochondrial hsp70 from its membrane anchor requires ATP binding rather than ATP hydrolysis. *Protein Sci.* **5**, 759–767 (1996).
56. Vasudevan, D., Chua, E.Y. & Davey, C.A. Crystal structures of nucleosome core particles containing the '601' strong positioning sequence. *J. Mol. Biol.* **403**, 1–10 (2010).
57. Dyer, P.N. *et al.* Reconstitution of nucleosome core particles from recombinant histones and DNA. *Methods Enzymol.* **375**, 23–44 (2004).
58. Huynh, V.A., Robinson, P.J. & Rhodes, D. A method for the *in vitro* reconstitution of a defined "30 nm" chromatin fibre containing stoichiometric amounts of the linker histone. *J. Mol. Biol.* **345**, 957–968 (2005).
59. Wong, I. & Lohman, T.M. A double-filter method for nitrocellulose-filter binding: application to protein-nucleic acid interactions. *Proc. Natl. Acad. Sci. USA* **90**, 5428–5432 (1993).

doi:10.1038/nsmb.2457

Supplementary Figures

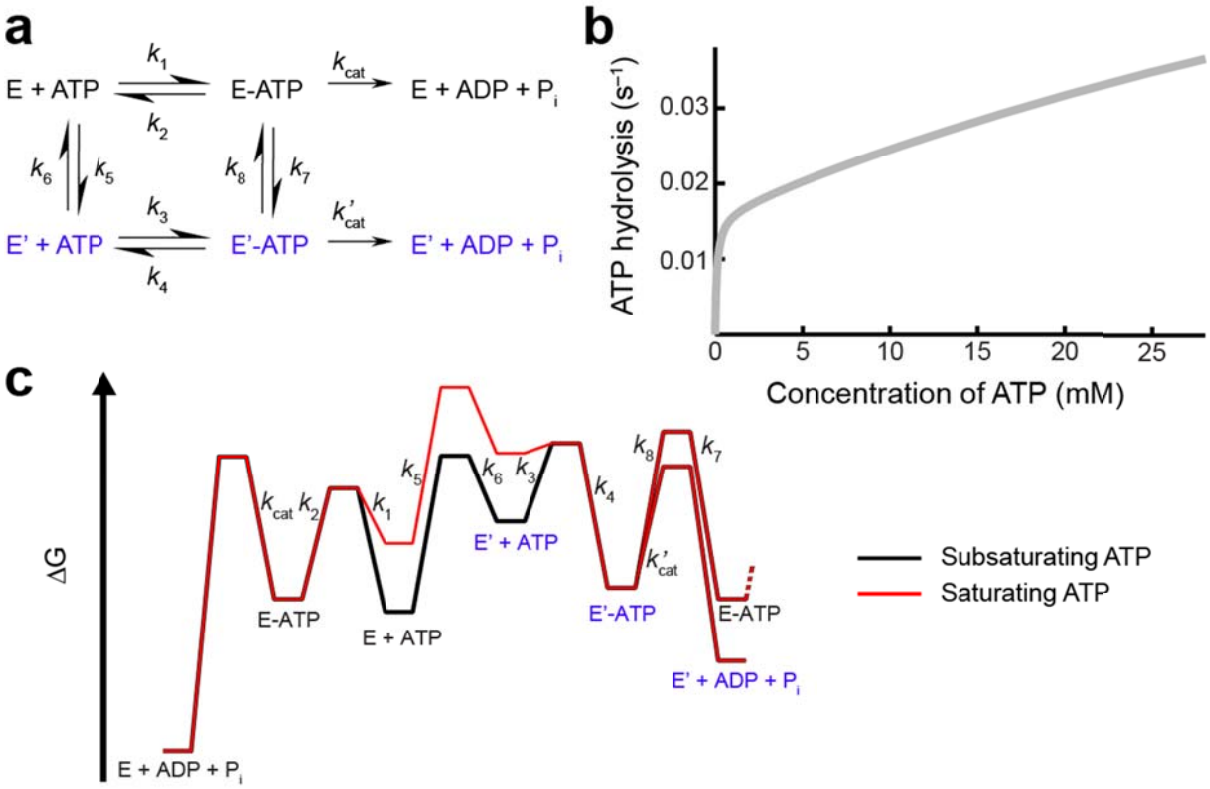

Supplementary Figure 1: The presence of two ISWI conformations can result in a biphasic ATP concentration dependence of ATP hydrolysis. (**a**) A simple reaction scheme in which the enzyme exists in two conformations, E and E', each being able to bind and hydrolyze ATP with different rate constants. (**b**) Modeling of the scheme in **a** showed that a biphasic ATP concentration dependence closely resembling the data shown in Figure 1a could be obtained (k_{cat} = 0.015 s^{-1}, k'_{cat} = 1 s^{-1}, k_1 = 10^5 M^{-1} s^{-1}, k_2 = 10 s^{-1}, k_3 = 10^9 M^{-1} s^{-1}, k_4 = 10^{-2} s^{-1}, k_5 = 10^{-3} s^{-1}, k_6 = 10^5 s^{-1}, k_7 = 10^{-4} s^{-1}, k_8 = 10^{-3} s^{-1}). Shown is an example in which both enzyme conformations had strongly different affinities for ATP. Note that many solutions resulted in biphasic behavior, not all of which required different ATP affinities (to produce a biphasic ATP concentration dependence, the ATP affinities of E and E' may or may not be similar to each other, E and E' may or may not have similar ATP turnover rates - k_{cat} or k'_{cat} may even become zero -, the ATP binding rate constants k_1 and k_3 may or may not assume similar values and the equilibration between E <=> E' and E-ATP <=> E'-ATP may or may not be similarly fast). Solutions that produce biphasic curves, however, required the four species E, E', E-ATP and E'-ATP to be present and to interconvert (mathematical derivation not shown). All solutions that produced a biphasic ATP response exhibited an ATP-concentration dependent change in the flux through the reaction scheme, i.e., different intermediates were populated due to a change in the rate limiting step (illustrated exemplary in the next panel). (**c**) Free energy profiles using the rate constants from the previous panel. With subsaturating concentrations of ATP (black line), E + ATP is the ground state of the reaction. E and ATP react to E-ATP, and ISWI then hydrolyzes ATP via k_{cat}. With saturating concentrations of ATP (red line), E + ATP quickly reacts to E-ATP. Since k_{cat} is too slow to hydrolyze all ATP immediately, some of the E-ATP reacts via k_7 to E'-ATP from where ATP is quickly hydrolyzed via k'_{cat}.

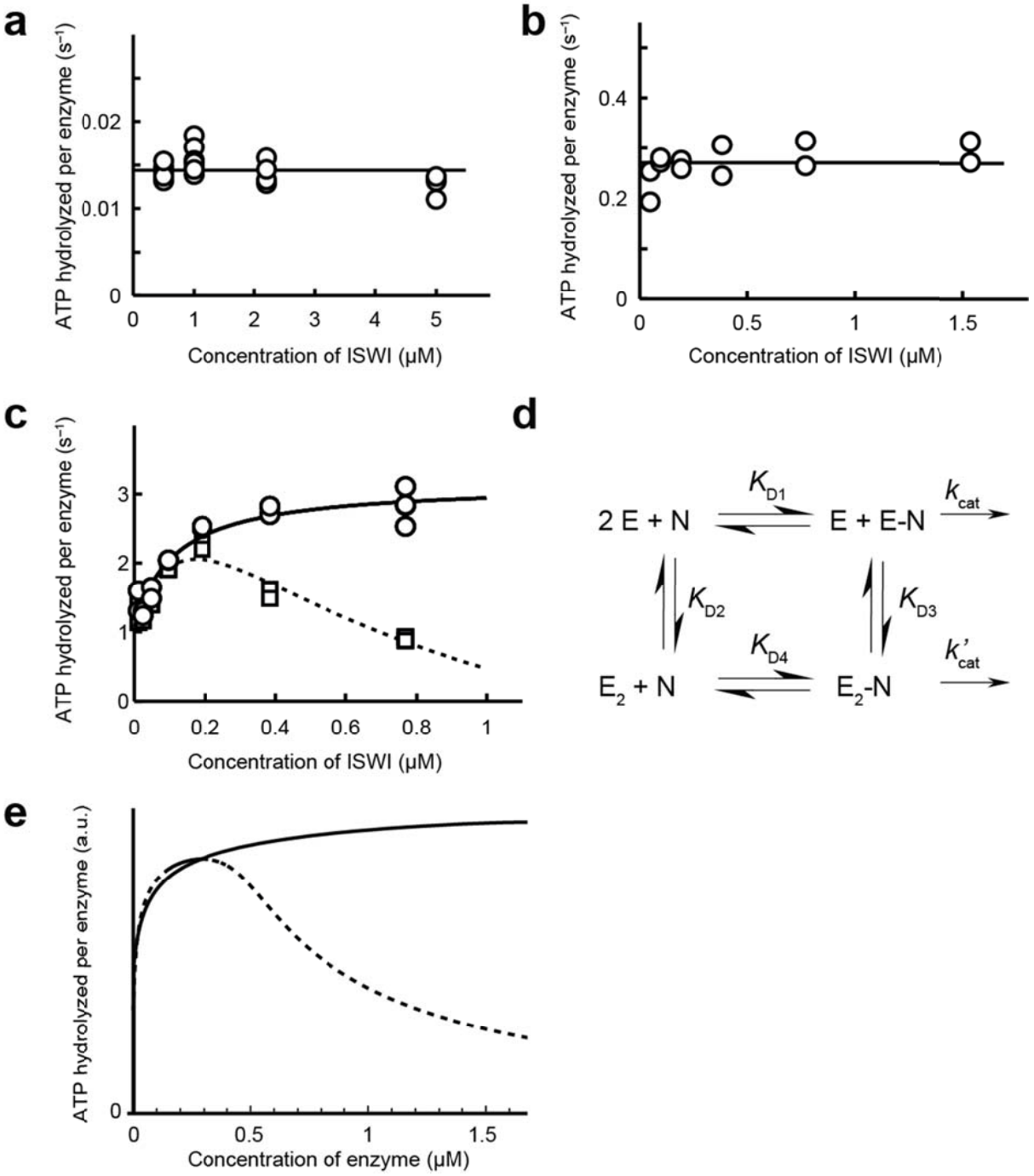

Supplementary Figure 2: Enzyme concentration dependence of ATP hydrolysis by $ISWI_{FL}$. (**a**) ATP hydrolysis by ligand-free $ISWI_{FL}$ was independent of the enzyme concentration between 0.5 and 5 µM. The biphasic ATP concentration dependence (**Fig. 1a**) therefore could not be caused by possible multimerization of ISWI. The assay was performed with 7 mM ATP in 100 mM Mg^{2+}. (**b**) ATP hydrolysis of DNA-bound $ISWI_{FL}$ remained constant between 0.05 to 1.5 µM enzyme, demonstrating that the ATPase signal was independent of possible enzyme multimerization. The assay was performed with saturating concentrations of 59-bp DNA and 3 mM ATP in 1.5 mM free Mg^{2+}. (**c**) The chromatin-stimulated reaction showed a pronounced dependence on the $ISWI_{FL}$ concentration. Two concentrations of chromatinized plasmid DNA were used (dashed line: 0.02 mg/mL, solid line: 0.1

mg/mL, referring to the DNA content). Increasing ATPase rates between 0 and 0.2 µM $ISWI_{FL}$ were consistent with enzyme dimerization on nucleosomes and subsequent enzyme activation[2]. The decreasing activity observed for the lower chromatin concentration above 0.2 µM $ISWI_{FL}$ was well explained by out-titration of available ISWI binding sites on chromatin. The data were collected with 3 mM ATP and 1.5 mM free Mg^{2+}. (**d**) Simple reaction scheme to explain the data shown in **c**. A single enzyme (E) bound to a nucleosome (N) hydrolyzes ATP with a different rate constant (k_{cat}) than an enzyme dimer (k'_{cat}). (**e**) *In silico* modeling of the reaction scheme in **d** recapitulated the features of the curves in **c**. Simulations were run for two nucleosome concentrations (0.2 µM, dashed line; 1 µM, solid line) with $K_{D1} = 10^{-1}$ µM, $K_{D2} = 10$ µM, $K_{D3} = 10^{-2}$ µM, $K_{D4} = 10^{-4}$ µM and $k'_{cat} = 4\ k_{cat}$.

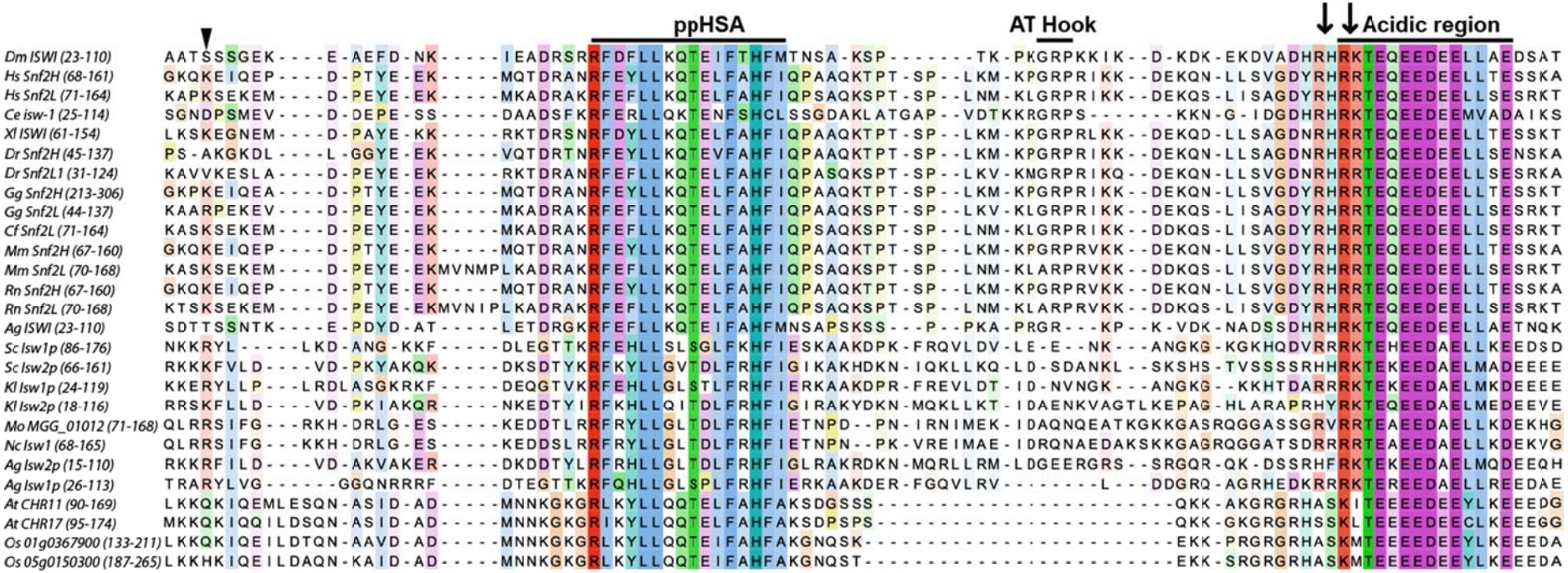

Supplementary Figure 3: Alignment of the N-terminal region of ISWI homologs from various organisms. Two highly conserved motifs exist: an acidic motif and the ppHSA motif, named so because it shares homology with the region after the post-HSA domain found in other family of remodelers (data not shown)[1]. The alignment is cut off at the C-terminal side before 'motif Q' of Snf2-type ATPases begins[3]. An AT hook ('GRP') has been previously described[4], but it is comparatively poorly conserved. The arrowhead points to the first amino acid included in $ISWI_{26–648}$. Arrows indicate tryptic cleavage sites obtained specifically in the DNA-bound conformation (**Fig. 3a**). *Dm: Drosophila melanogaster, Hs: Homo sapiens, Ce: Caenorhabditis elegans, Xl: Xenopus laevis, Dr: Danio rerio, Gg: Gallus gallus, Cf: Canis familiaris, Mm: Mus musculus, Rn: Rattus norvegicus, Ag: Anopheles gambiae, Sc: Saccharomyces cerevisiae, Kl: Kluyveromyces lactis, Mo: Magnaporthe oryzae, Nc: Neurospora crassa, Ag: Ashbya gossypii, At: Arabidopsis thaliana, Os: Oryza sativa.* Amino acid numbers are given in parenthesis. The color intensity is indicative of the level of conservation. The alignment was performed with T-Coffee (www.ebi.ac.uk/Tools/msa/tcoffee/), and the figure was prepared with Jalview 2.7 (www.jalview.org/).

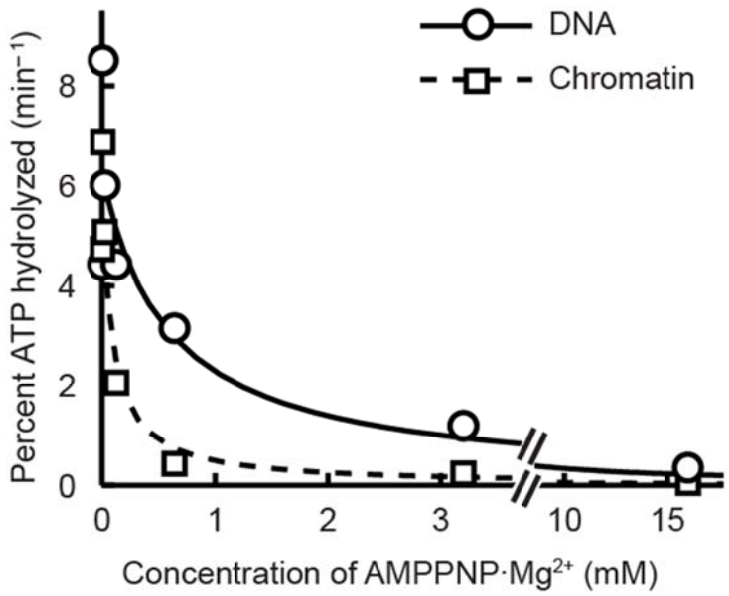

Supplementary Figure 4: The nucleotide affinity increased six-fold if ISWI was bound to chromatin instead of DNA. The affinity of the non-hydrolyzable ATP analog AMPPNP was measured in a competition experiment using ATP hydrolysis as readout. Saturating concentrations of 39-bp duplex DNA (20 µM) or chromatinized plasmid DNA (0.08 mg/mL) were incubated with $ISWI_{FL}$ (80 nM or 10 nM, respectively) and varying concentrations of AMPPNP. The reaction was initiated with 1 µM ATP. The data were fit to a binding isotherm and yielded K_i values of 570 µM (solid line) and 90 µM (dashed line). The affinity for ADP was similarly increased (data not shown). The ~six-fold effect on the K_i was larger than the ~two-fold effect on $K_{M,obs}$ (**Suppl. Table 1**). This discrepancy indicated that the $K_{M,obs}$ values did not directly reflect the affinity for ATP.

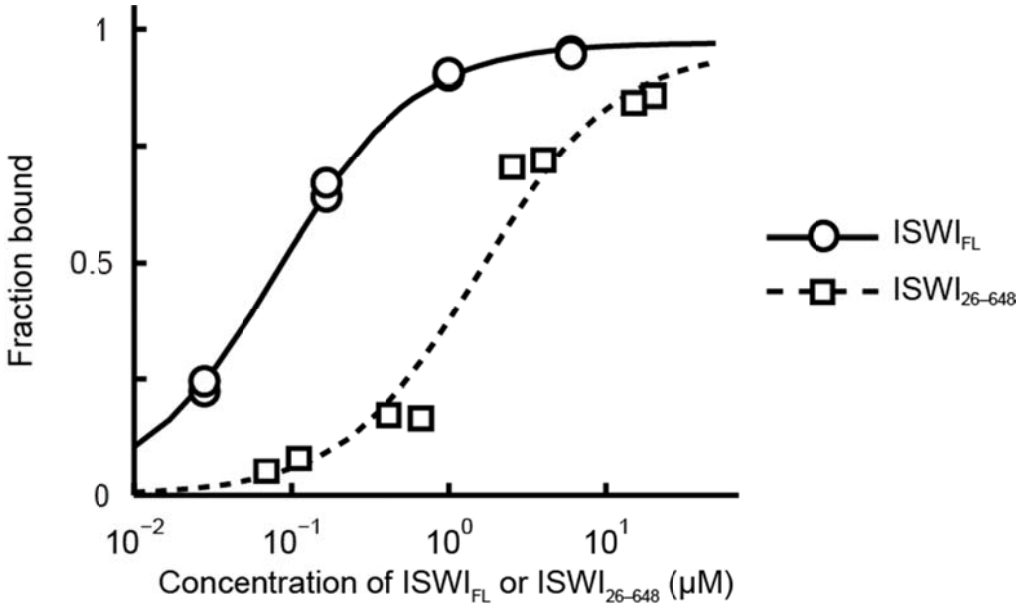

Supplementary Figure 5: Deletion of the HSS domain led to a decreased DNA affinity but did not abolish DNA binding. Binding of trace amounts of duplex DNA to $ISWI_{FL}$ or $ISWI_{26–648}$ was followed in a double-filter DNA binding assay[5]. Lines are fits of the data to a simple binding isotherm yielding K_D = 0.08 μM (solid line) and K_D = 1.6 μM (dashed line).

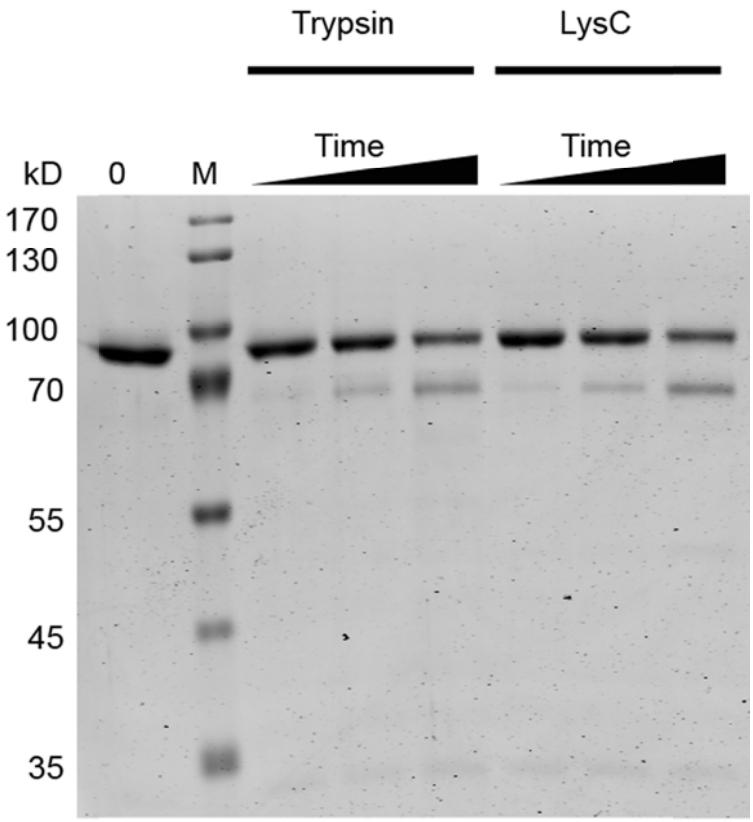

Supplementary Figure 6: Trypsin and LysC cleaved the same residues in DNA-free $ISWI_{26–648}$. Proteolytic fragments of $ISWI_{26–648}$ generated by trypsin and LysC (20 nM and 17 nM, respectively) after 5, 15 and 60 min were separated by SDS-PAGE and stained with Coomassie Blue. The identical mobility of the predominant cleavage products suggested that trypsin cleaved DNA-free $ISWI_{26–648}$ next to a lysine, not an arginine residue. 0: Undigested sample. M: Molecular weight marker.

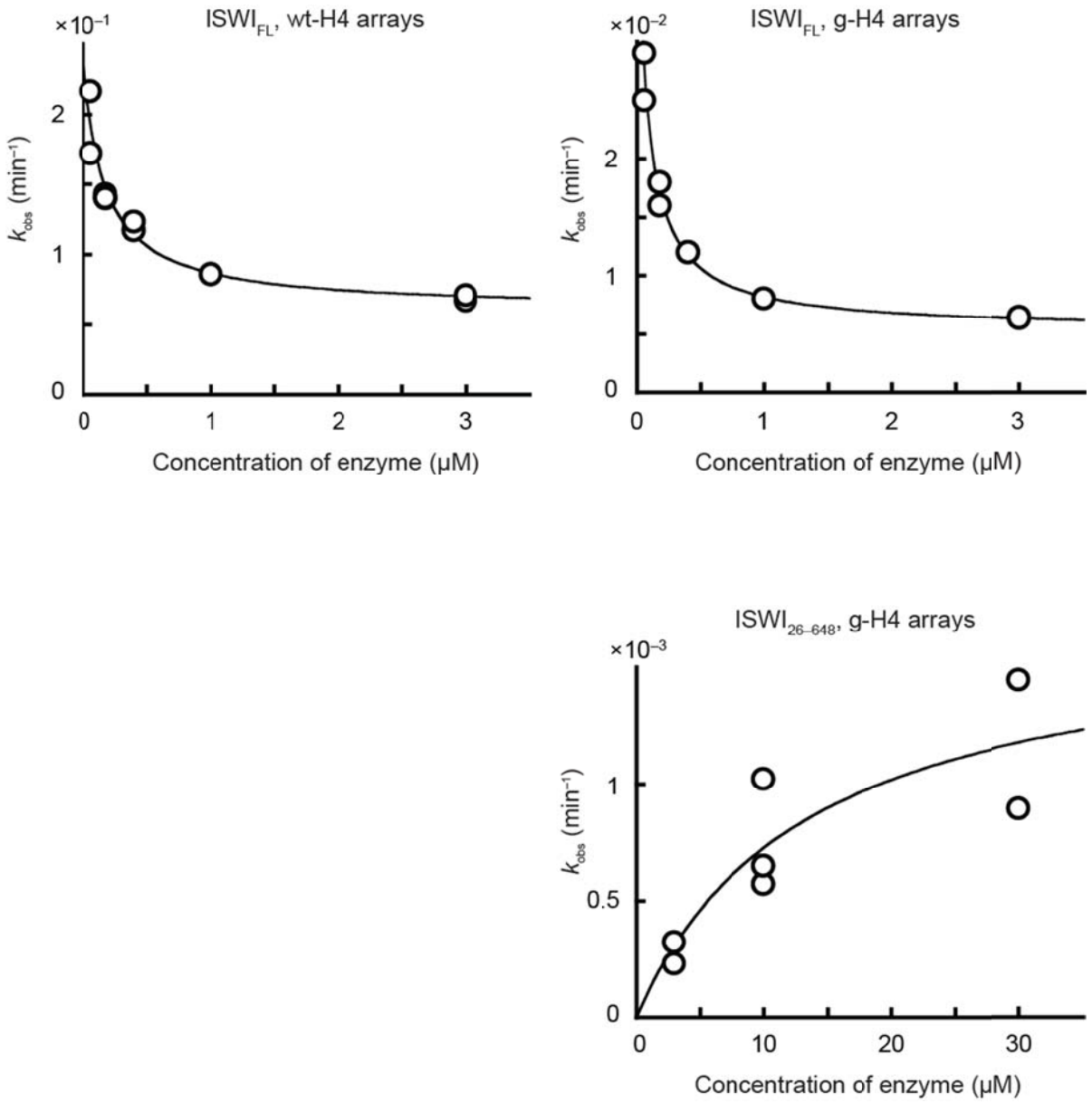

Supplementary Figure 7: Determination of the maximal remodeling velocities of ISWI$_{FL}$ and ISWI$_{26–648}$ on wt-H4 and g-H4 arrays. As described by others, the remodeling activities *decreased* with increasing enzyme concentration for ISWI$_{FL}$ (http://www.epigenesys.eu/; Protocol PROT24). To obtain the maximal remodeling velocities ($k_{obs,max}$) for ISWI$_{FL}$, we corrected for this decrease by fitting the data to inverse binding isotherms (see Methods), extrapolating back to (low) enzyme concentrations where this effect was not present. $k_{obs,max}$ for ISWI$_{26–648}$ remodeling of g-H4 arrays was determined as before (**Fig. 6d**). Data points within each graph were from multiple independent experiments.

Supplementary Tables

Supplementary Table 1: ATPase parameters of $ISWI_{FL}$ and $ISWI_{26–648}$ [a]

		TLC assay	NADH ox. coupled assay		
		$k_{cat}/K_{M,obs}$	$k_{cat}/K_{M,obs}$	$k_{cat,\,obs}$	$K_{M,obs}$
		($M^{-1}\,s^{-1}$)	($M^{-1}\,s^{-1}$)	(s^{-1})	(mM)
$ISWI_{FL}$	DNA	$(3.2 \pm 0.8)\times10^3$	$(1.5 \pm 0.4)\times10^3$	0.22 ± 0.04	0.12 ± 0.03
	NCP	$(5 \pm 2)\times10^4$*	N.d.[b]	1.9 ± 0.8	0.04 ± 0.03[c]
	Chromatin	$(3 \pm 1)\times10^4$	$(3.7 \pm 0.1)\times10^4$	1 to 3[d]	0.05 ± 0.02

		$k_{cat}/K_{M,obs}$[e]
		($M^{-1}\,s^{-1}$)
$ISWI_{26–648}$	DNA	$(4.1 \pm 0.6)\times10^3$
	NCP	$(9 \pm 4)\times10^4$*
	Chromatin	$(7 \pm 5)\times10^4$

[a]: Compared to Table 1 in the main text, a reaction buffer containing a lower Mg^{2+} concentration (1.5 mM) was used to prevent aggregation of chromatin. All reported values were obtained with saturating ligand concentrations. DNA reactions contained a 39-bp DNA duplex (NADH oxidation coupled assay) or 147-bp DNA (TLC assay), NCP reactions nucleosome core particles assembled on the 147-bp Widom-601 sequence, and chromatin reactions 25-mer nucleosomal arrays (TLC assay) or polynucleosomes assembled on plasmid DNA (NADH assay). Where indicated (asterisk), errors are min and max values of two independent measurements. Otherwise, errors are standard deviations of at least three independent measurements.
[b]: N.d.: Not determined.
[c]: Value calculated from $k_{cat,obs}$ and $k_{cat}/K_{M,obs}$.
[d]: Values varied with the enzyme concentration (**Suppl. Fig. 2c**).
[e]: All values measured by the TLC ATPase assay.

Supplementary Table 2: (a) Oligonucleotides[a]; (b) oligopeptides used in the study[b]

	Name	Sequence
a	39-bp DNA duplex	5'-TGCATGTATTGAACAGCGACTCGGGTTATGTGATGGACC
	59-bp DNA duplex	5'-ATACATCCTGTGCATGTATTGAACAGCGACTCGGGTTATGTGATGGACCCTATACGCGG
b	H4 tail peptide	TGRGKGGKGLGKGGAKRHRKVLRD
	Scrambled peptide 1	BGARLDGRKGHGGRLKGKVRGGKK
	Scrambled peptide 2	KLRRGGXGDVKTGKLGGRKAGRGH

[a]: Sequences of only one of the two strands per DNA duplex are shown.
[b]: X indicates an acetylated lysine residue. B stands for the unnatural amino acid *p*-benzoyl-*p*-phenylalanine, which connects to the neighbouring amino acids via a regular peptide bond.

Supplementary Note

Additional scenarios explaining a biphasic ATP concentration dependence of ATP hydrolysis

1) *"ISWI is mostly dimerized in solution under assay conditions and each subunit has a different K_M for ATP."*

   This possibility is ruled out by the observation that DNA-free ISWI is in a monomeric state in solution as measured by multiple angle light scattering by us (data not shown) and by analytical ultracentrifugation by others[2].

2) *"A small fraction of ISWI is dimerized in solution under assay conditions, and the monomer and the dimer have different K_M values for ATP."*

   One would expect that more dimer forms with increasing enzyme concentrations and that the observed reaction velocity would consequently change as well. This expectation is not consistent with experimental results (**Suppl. Fig. 2a,b**).

3) *"ISWI preparations contain contaminating DNA. DNA-free and the DNA-bound ISWI have a different K_M for ATP."*

   Treatment with nucleases and extensive purification of $ISWI_{FL}$ using five consecutive chromatography steps (including size exclusion chromatography in 2 M salt) did not abolish the biphasic behavior seen in Figure 1a. Moreover, we did not observe changes of the biphasic shape upon a jump in the ionic strength of the buffer (from 1.5 mM to 100 mM Mg^{2+}), which should drastically weaken protein-DNA interactions (data not shown). Finally, $ISWI_{1–697}$ and $ISWI_{26–648}$ also exhibited a biphasic response to the ATP concentration (**Fig. 1b** and data not shown) although they intrinsically bound DNA with much weaker affinity than $ISWI_{FL}$ (**Suppl. Fig. 5**).

4) *"Proteolysis fragments of ISWI are present, and they have a different K_M for ATP."*

   The extensive purification discussed above argued against this possibility. Moreover, constructs lacking the entire C-terminus ($ISWI_{1–697}$ and $ISWI_{26–648}$) still showed the biphasic response to variation of the ATP concentration, making it unlikely that the same contaminants were present in all enzyme preparations (**Fig. 1b** and data not shown).

5) *"ISWI possesses a second, allosteric binding site for ATP."*

   Neither structural nor biochemical evidence exists for ISWI or related enzymes to support a second, allosteric binding site.

6) *"A fraction of ISWI is misfolded and therefore nearly inactive".*

   Active site titration experiments with 39-bp long DNA duplexes refuted the possibility that a majority of $ISWI_{26–648}$ was misfolded to the extent that DNA could not bind and stimulate ATP hydrolysis (data not shown). Our active site titration experiments were, however, not sensitive enough to detect a minor fraction of misfolded protein. If this minor fraction were responsible for one or the other catalytic phase of the biphasic ATPase curve, its specific ATPase activity would however be considerable as the following consideration shows. In the biphasic ATPase curve, the

first phase contributed 0.014 s^{-1} and the second phase >0.046 s^{-1} to the amplitude (**Table 1**). If, for example, 10% misfolded, nearly inactive protein were present, its specific activity would be 0.14 s^{-1} (= 10 × 0.014 s^{-1}) or >0.46 s^{-1} (= 10 × 0.046 s^{-1}). These values approach the DNA-stimulated $k_{cat,obs}$ of 0.51s^{-1}. The hypothetical misfolded fraction can therefore not be considered "nearly inactive".

Why can $ISWI_{26–648}$ not distinguish nucleosomes from free DNA in presence of saturating ATP?

The $k_{cat}/K_{M,obs}$ of $ISWI_{26–648}$ was markedly (17- to 23-fold) stimulated by NCPs and nucleosomal arrays relative to DNA (**Fig. 3a,b**) whereas the $k_{cat,obs}$ apparently was not (data not shown). Two scenarios could explain these observations. The first scenario is discussed in the main text. In this scenario, $ISWI_{26–648}$ would recognize the DNA component of the nucleosome, leading to DNA-like stimulation, but most enzyme molecules - at steady-state - would not find the proper site at SHL2. Support for this scenario came from the observation that $ISWI_{26–648}$ could only poorly discriminate between free DNA and nucleosomes even under subsaturating ATP concentrations. $ISWI_{FL}$, on the other hand, was much less prone to unproductive binding because the HSS domain strongly increased the specificity for nucleosomes (**Fig. 3c**).

The second scenario, in contrast, posits that all $ISWI_{26–648}$ molecules bind productively at SHL2 of the nucleosome. Lack of stimulation of $k_{cat,obs}$ therefore cannot be explained by unproductive binding elsewhere on nucleosomal DNA in this model. If true, $K_{M,obs}$ for $ISWI_{26–648}$ would have to decrease by 17- to 23-fold, such that $k_{cat,obs}$ devided by $K_{M,obs}$ would yield a value that is 17- to 23-fold larger relative to DNA. Evidence against this scenario came from steady-state ATPase parameters of $ISWI_{FL}$. The $K_{M,obs}$ of $ISWI_{FL}$ was only modestly decreased (two- to three-fold; **Suppl. Table 1**). Given the high similarity of the ATPase parameters of $ISWI_{FL}$ and $ISWI_{26–648}$, the second scenario seemed unlikely.

Supplementary References

1. Szerlong, H. et al. The HSA domain binds nuclear actin-related proteins to regulate chromatin-remodeling ATPases. *Nat Struct Mol Biol* **15**, 469-76 (2008).
2. Racki, L.R. et al. The chromatin remodeller ACF acts as a dimeric motor to space nucleosomes. *Nature* **462**, 1016-21 (2009).
3. Flaus, A., Martin, D.M., Barton, G.J. & Owen-Hughes, T. Identification of multiple distinct Snf2 subfamilies with conserved structural motifs. *Nucleic Acids Res* **34**, 2887-905 (2006).
4. Aravind, L. & Landsman, D. AT-hook motifs identified in a wide variety of DNA-binding proteins. *Nucleic Acids Res* **26**, 4413-21 (1998).
5. Wong, I. & Lohman, T.M. A double-filter method for nitrocellulose-filter binding: application to protein-nucleic acid interactions. *Proc Natl Acad Sci U S A* **90**, 5428-32 (1993).